Geochemistry Geophysics Geosystems G3
AN ELECTRONIC JOURNAL OF THE EARTH SCIENCES
Published by AGU and the Geochemical Society

Article
Volume 5, Number 11
6 November 2004
Q11005, doi:10.1029/2004GC000731
ISSN: 1525-2027

Oblique rifting and segmentation of the NE Gulf of Aden passive margin

Marc Fournier
Laboratoire de Tectonique, CNRS UMR 7072, Université Paris 6, Case 129, 4 place Jussieu, 75252 Paris Cedex 5, France (marc.fournier@lgs.jussieu.fr)

Nicolas Bellahsen
Department of Geological and Environmental Sciences, Stanford University, 450 Serra Mall, Stanford, California 94305-2115, USA

Olivier Fabbri
Département de Géosciences, Université de Franche-Comté, 16 route de Gray, 25030 Besançon, France

Yanni Gunnell
Laboratoire de Géographie Physique, CNRS UMR 8591, Université Paris 7, Case 7001, 2 place Jussieu, 75251 Paris Cedex 5, France

[1] The Gulf of Aden is a young, obliquely opening, oceanic basin where tectonic structures can easily be followed and correlated from the passive margins to the active mid-oceanic ridge. It is an ideal laboratory for studies of continental lithosphere breakup from rifting to spreading. The northeastern margin of the Gulf of Aden offers the opportunity to study on land the deformation associated with oblique rifting over a wide area encompassing two segments of the passive margin, on either side of the Socotra fracture zone, exhibiting distinct morphologic, stratigraphic, and structural features. The western segment is characterized by an elevated rift shoulder and large grabens filled with thick synrift series, whereas the eastern segment exhibits low elevation and is devoid of major extensional structures and typical synrift deposits. Though the morphostructural features of the margin segments are different, the stress field analysis provides coherent results all along the margin. Four directions of extension have been recognized and are considered to be representative of two tensional stress fields with permutations of the horizontal principal stresses σ_2 and σ_3. The two dominant directions of extension, N150°E and N20°E, are perpendicular to the mean trend of the Gulf of Aden (N75°E) and parallel to its opening direction (N20°E–N30°E), respectively. Unlike another study in the western part of the gulf, our data suggest that the N150°E extension stage is older than the N20°E extension stage. These conflicting chronologies, which are nowhere unambiguously established, suggest that the two extensions coexisted during the rifting. On-land data are compared with offshore data and are interpreted with reference to oblique rifting. The passive margin segmentation represents a local accommodation of the extensional deformation in a homogeneous regional stress field, which reveals the asymmetry of the rifting process. The first-order segmentation of the Sheba Ridge is inherited from the prior segmentation of the passive margin.

Components: 11,565 words, 10 figures, 1 table.

Keywords: continental breakup; Gulf of Aden; oblique rifting; paleostress; passive margin; segmentation.

Index Terms: 8105 Tectonophysics: Continental margins and sedimentary basins (1212); 8109 Tectonophysics: Continental tectonics—extensional (0905); 8164 Tectonophysics: Stresses—crust and lithosphere.

Received 21 March 2004; **Revised** 23 August 2004; **Accepted** 20 September 2004; **Published** 6 November 2004.

Fournier, M., N. Bellahsen, O. Fabbri, and Y. Gunnell (2004), Oblique rifting and segmentation of the NE Gulf of Aden passive margin, *Geochem. Geophys. Geosyst.*, *5*, Q11005, doi:10.1029/2004GC000731.

1. Introduction

[2] Oblique rifting is the process through which the relative displacement on either side of a rift zone is not perpendicular but oblique to the trend of the rift zone. The faulting pattern resulting from oblique rifting has been investigated with empirical data from oceanic and continental rifts [*Dauteuil and Brun*, 1993, 1996; *McAllister et al.*, 1995; *Dauteuil et al.*, 2001; *Acocella and Korme*, 2002; *Clifton and Schlische*, 2003] and by means of analogue [*Withjack and Jamison*, 1986; *Tron and Brun*, 1991; *Dauteuil and Brun*, 1993; *McClay and White*, 1995; *Bonini et al.*, 1997; *Clifton et al.*, 2000; *Mart and Dauteuil*, 2000], analytic [*Withjack and Jamison*, 1986; *Tuckwell et al.*, 1996; *Abelson and Agnon*, 1997], and numeric [*Tuckwell et al.*, 1998] models. These studies show that oblique rifting is accommodated by both normal and strike-slip faults whose relative proportions and orientations depends on rifting obliquity, which is the angle between the normal to the rift trend and the direction of displacement. When oblique continental rifts evolve into oblique oceanic spreading ridges, they may take one of two configurations [*Atwater and Macdonald*, 1977; *Abelson and Agnon*, 1997]: either a configuration involving a continuous (without transform fault) oblique spreading axis or a configuration with a spreading axis segmented by transform faults. The Reykjanes Ridge, close to the Iceland hot spot, and the westernmost Sheba Ridge in the Gulf of Aden [*Tamsett and Searle*, 1988; *Dauteuil et al.*, 2001], close to the Afar hot spot, belong to the first category of spreading ridges, whereas most of the slow spreading centers, including the Sheba Ridge east of 46°E, belong to the second category. Like the oceanic ridges, the continental rifts and the passive margins are segmented, but the relationship between the segmentations is poorly understood [*Hayward and Ebinger*, 1996]. In the Gulf of Aden, the first-order segments of the ridge are arranged en echelon and connected by NE-striking transform faults (Figure 1) [*Laughton*, 1966; *Matthews et al.*, 1967]. The present en echelon pattern is mirrored in the stepped shape of the continental margins of Arabia and Somalia, which implies that the transform faults are the result of initial offsets between spreading ridge segments which existed at the beginning of the oceanic accretion. The fracture zones, i.e., the inactive continuations of the transform faults, do not continue into the continental lithosphere but abut against the continental platform, as predicted by *Wilson* [1965]. Here, within the general problem of oblique rifting and segmentation, the following questions are examined: (1) what is the record of oblique rifting on passive margins? (2) How is the segmentation expressed in passive margins? (3) Is oceanic ridge segmentation inherited from prior passive margin segmentation?

[3] The Gulf of Aden is a type example of an obliquely opening oceanic basin [*Cochran*, 1981; *Withjack and Jamison*, 1986]. Because it is a young basin, structures can be followed from the passive margins to the active mid-oceanic ridge, and the two conjugate margins can be precisely correlated. Moreover, the northeastern passive margin of the Gulf of Aden offers the opportunity to study on land the deformation associated with oblique rifting over a wide area encompassing two margin segments located on either side of the Socotra fracture zone. In the following, we present the results of a structural analysis conducted in the Cenozoic series of this area to characterize the synrift deformation by the observation and measurement of the motion along major and minor faults. In addition, new bathymetric and seismic data obtained offshore to the south of our study area allow us to widen the discussion on the mode of opening of the Gulf of Aden.

2. Geodynamic Setting

2.1. Oblique Opening of the Gulf of Aden

[4] The opening of the Gulf of Aden was accomplished through sea floor spreading along the mid-oceanic Sheba Ridge. The present-day accretion rate at the Sheba Ridge progressively increases from west (1.6 cm/yr along N37°E at the entrance of the gulf of Tadjura, 12°N and 43.4°E) to east (2.3 cm/yr along N23°E at the Arabia-India-Somalia triple junction, 14.5°N and 56.4°E). At the longitude of Dhofar (14.4°N and 53°E), the spreading rate is 2.2 cm/yr along N25°E [*Jestin et al.*, 1994; *Fournier et al.*, 2001b]. Hence the mean opening direction of the Gulf of Aden, N25°E, is oblique to its mean orientation, N75°E. The linearity of the transform

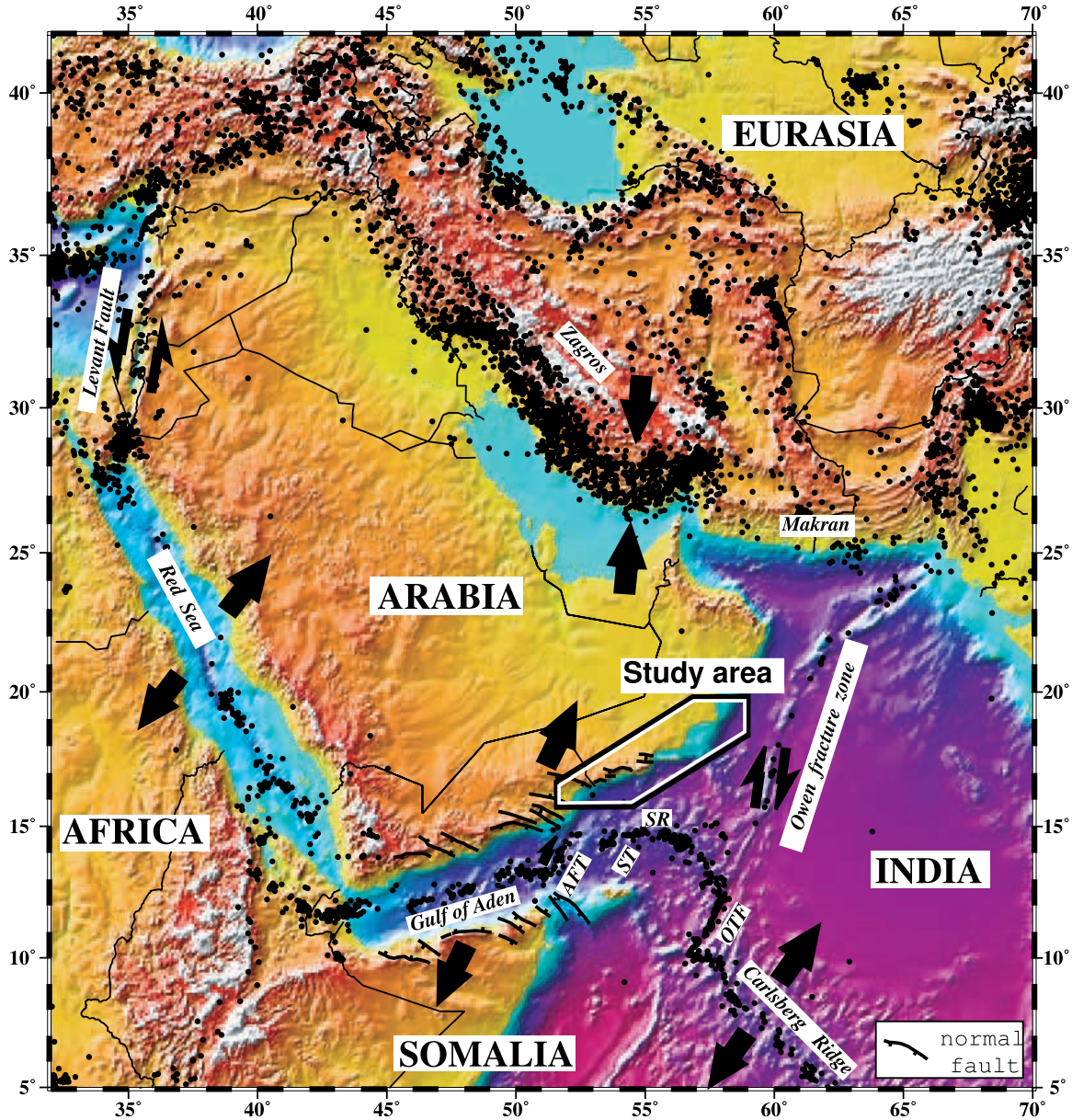

Figure 1. Geodynamical setting of the Gulf of Aden and the Arabian plate. Topographic and bathymetric map is after *Sandwell and Smith* [1997], and shallow seismicity is since 1973 (focal depth <50 km; magnitude >2; USGS/NEIC database). Black arrows represent plate relative motions. The N100°–110°E grabens bounded by normal faults arranged obliquely to the N75°E mean trend of the Gulf of Aden are shown. AFT, Alula-Fartak transform fault; OTF, Owen transform fault; SR, Sheba Ridge; ST, Socotra transform fault.

faults indicates that the direction of opening has remained unchanged since the initial breakup of the two plates. In the eastern part of the gulf, the age of the inception of oceanic spreading has been recently reappraised from magnetic profiles of the Encens-Sheba cruise [*d'Acremont*, 2002; *Leroy et al.*, 2004]. The magnetic anomaly An 5d has been identified to the north and south of the Sheba Ridge axis, and gives an age of the start of spreading of at least 17.6 Ma instead of 12–13 Ma as previously proposed by *Cochran* [1981]. These results confirm those of *Sahota* [1990]. To the west of the Alula-Fartak transform fault, anomaly An 5c has been identified showing that the oceanic spreading has started at least 16 m.y. ago in the western part of the Gulf of Aden [*Sahota*, 1990; *Huchon and Khanbari*, 2003]. Oceanic spreading was preceded by rifting of the continental lithosphere which was initiated during the Oligocene and continued until the early Miocene [*Roger et al.*, 1989; *Watchorn et al.*, 1998]. Rifting in the Gulf of Aden led to the formation of a series of N100°E–N110°E grabens

arranged obliquely to the N75°E mean trend of the gulf [*Beydoun*, 1970, 1982; *Tamsett*, 1984; *Abbate et al.*, 1993; *Fantozzi*, 1996]. The en echelon left stepping arrangement of the synrift basins is consistent with the dextral component of oblique opening of the gulf.

2.2. Uplift History of the Gulf of Aden Margins: Insights From Apatite Fission Track Data

[5] The uplift history of the Gulf of Aden passive margins has been investigated through AFT analysis on rock samples of Archaean to Jurassic age in Yemen [*Menzies et al.*, 1997] and Somalia [*Abbate et al.*, 2001]. The AFT cooling ages are widely distributed across the two margins and indicate a complex cooling history which is interpreted in terms of discrete cooling or burial events, and differential denudation. In Yemen the margin experienced Oligocene (>30 Ma) cooling and unroofing coevally with the main extensional stage involving tilted fault blocks, which began at about 35 Ma [*Watchorn et al.*, 1998]. In Somalia a first phase of denudation at the margin occurred during the early Cretaceous, possibly related to a Jurassic to early Cretaceous episode of rifting, followed by a second phase which began in the late Oligocene, continued in the Miocene, and is attributable to the rifting of the Gulf of Aden [*Abbate et al.*, 2001].

[6] These data contrast with the AFT data of the southeastern Red Sea margin, which were reset during the major volcanism episode of the Yemen Large Igneous Province at 31–26 Ma [*Baker et al.*, 1996] and are consistent with rapid cooling and unroofing of the margin in the early Miocene (<25 Ma) coevally with the main phase of extension [*Menzies et al.*, 1997; *Ukstins et al.*, 2002; *Pik et al.*, 2003]. While the southeastern Red Sea margin developed in response to surface uplift and magmatism which was followed ca 5 m.y. later by extension and denudation, the Gulf of Aden margins have experienced tectonically driven Oligocene to early Miocene denudation in the absence of significant magmatism. In all cases, the uplift of the rift shoulders preceded the onset of seafloor spreading.

3. Segmentation of the Oman Margin of the Gulf of Aden: Morphologic and Structural Evidence

[7] The morphology of the Oman margin is different on either side of the Socotra fracture zone (Figure 1). The western part corresponds to the Dhofar region, and the eastern part to the Jiddat Arkad region (Figure 2). They are separated on land by the Jabal Qarabiyan fault, which strikes parallel to the Socotra fracture zone, but the two faults are not of the same type. The Jabal Qarabiyan fault appears as a pure normal fault in the field (see section 5.2.1), whereas the Socotra fracture zone is an ancient transform fault.

[8] In Dhofar the margin is dominated by a monoclinal plateau tilted a few degrees toward the north, made up of mainly Eocene carbonate platform. The plateau is bounded to the south by the south facing escarpments of Jabal al Qamar, Jabal Qara and Jabal Samhan (Figure 2), which rise up to 1800 m and define the northern shoulder of the rift. The Ashawq and Hasik main grabens and the Haluf and Sala'Afan minor grabens occur behind the main escarpment (Figure 2). The grabens are delimited by N70°E to N110°E trending fault scarps of plurikilometric extent well expressed in the topography, which reflect post-Eocene displacements. The two main grabens present an axial dip toward the east. The Proterozoic basement is exposed south of the Hasik graben and corresponds to a footwall block formed during the rifting. This uplifted block is bounded seaward (to the south) by the submerged portion of the extensional margin, and landward (to the north) by the Hasik graben.

[9] The topography of the margin is much smoother in the Jiddat Arkad region, which is nearly devoid of any rift shoulder. The plateau as far as Ra's Madrakah consists of a monotonous flat surface 200–300 m above sea level (Figure 2). No major extensional structure is observed on this segment of the margin, with the exception of the zone of coastal fault blocks stepping down into the sea around Sharbithat. The rift shoulder occurs at the Al Hallaniyah islands, which rise to 450 m and are bounded to the south by the submerged passive margin. Hence two margin segments characterized by different morphostructural features are recognized on either side of the Socotra fracture zone.

4. Contrasted Cenozoic Stratigraphic Units of Dhofar and Jiddat Arkad Regions

[10] In southern Oman, a carbonate succession up to 2000 m thick is exposed [*Platel and Roger*, 1989; *Roger et al.*, 1989; *Béchennec et al.*, 1993; *Robertson and Bamkhalif*, 2001]. The Cenozoic series includes the Hadhramaut, Dhofar, and Fars groups, which correspond to prerift, synrift and

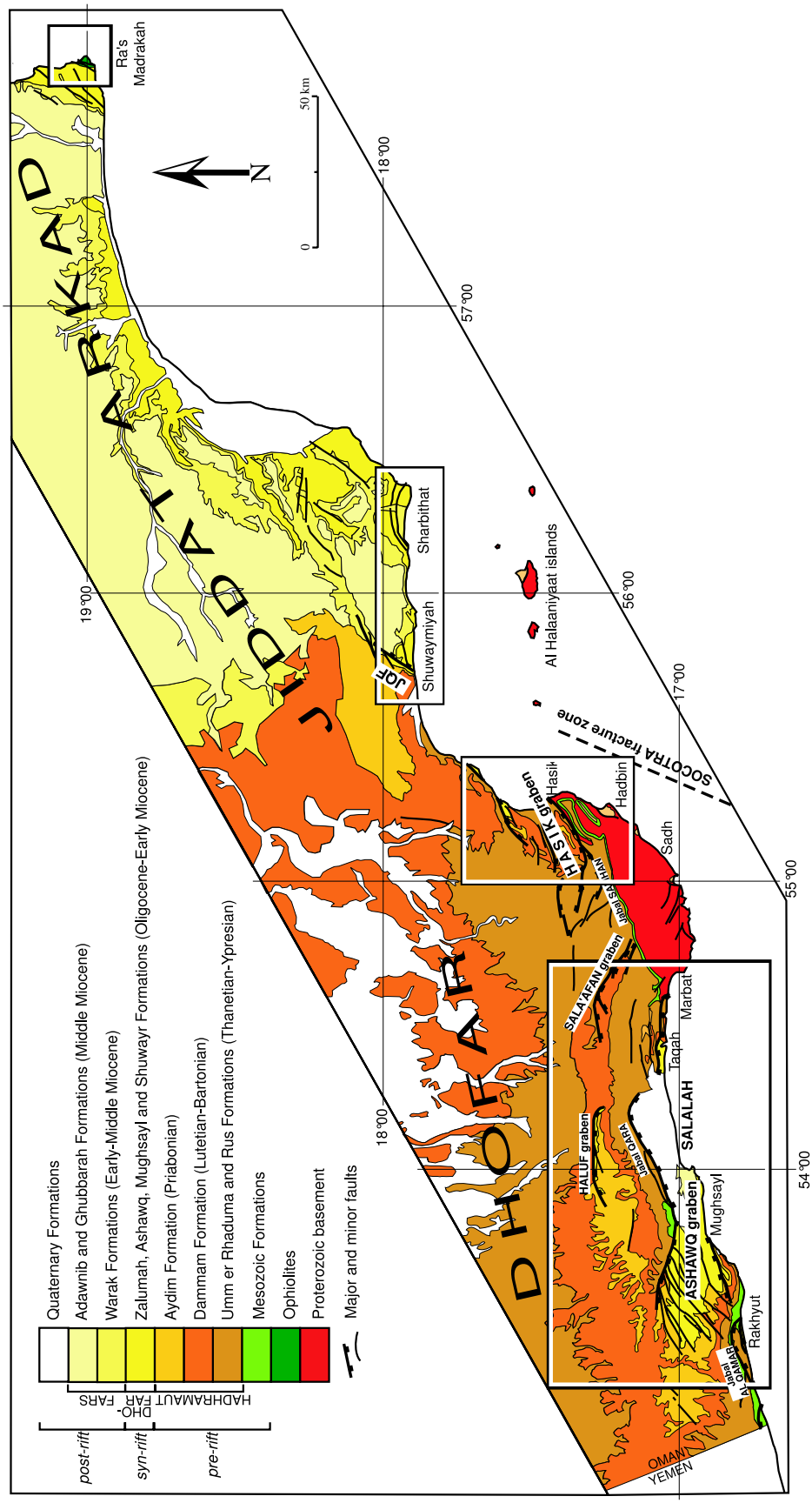

Figure 2. Structural map of Dhofar and Jiddat Arkad after the 1/250000 geological maps of Oman [*Platel et al.*, 1992a, 1992b, 1992c; *Roger et al.*, 1992] and location of the surveyed areas. JQF, Jabal Qarabiyan Fault.

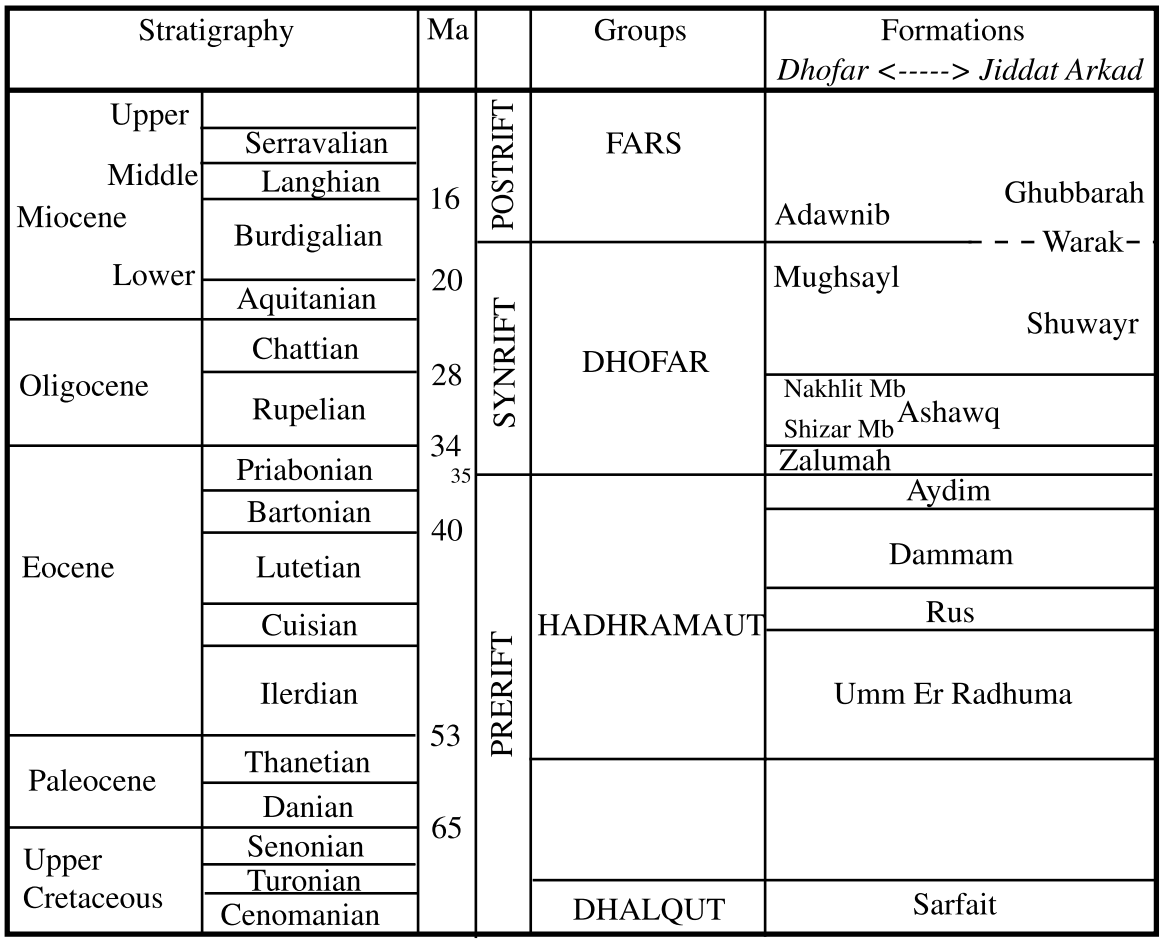

Figure 3. Stratigraphic synthesis of the Mesozoic and Cenozoic strata exposed in Dhofar and Jiddat Arkad (from *Roger et al.* [1989] and *Platel and Roger* [1989]).

postrift stages of deposition, respectively (Figure 3). Two distinct stratigraphic domains corresponding to the Dhofar and Jiddat Arkad areas can be distinguished. The western domain is dominated by the Eocene series of the Hadramaut Group, the Dhofar and Fars groups being restricted to the synrift grabens and the Salalah plain, whereas the eastern domain is dominated by the formations of the Fars Group (Figure 2).

[11] In Dhofar, the prerift Hadhramaut Group rests unconformably upon Cretaceous strata, which in turn overlie the Proterozoic basement exposed east of Marbat (Figures 2 and 3). The Hadhramaut Group consists of carbonate units, including the massive limestone of the Umm Er Radhuma Formation (up to 600 m thick). The synrift Dhofar Group, unconformably deposited on the Hadhramaut Group, consists of lacustrine limestone at the base (100 m), overlain by platform limestone (Ashawq Formation, 600 m), which passes laterally at top to the overlying, chalky calci-turbidic deposits of the late Oligocene to early Miocene Mughsayl Formation (700 m thick beneath the Salalah plain [*Platel et al.*, 1992c]). The slope deposits of the Mughsayl Formation, which include megabreccia, debris flows, and olistolitic material transported from the adjoining shelf, result from the collapse and subsidence of the margin and correspond to deeper depositional environments. The postrift Fars Group is restricted to a narrow zone following the coast line, and is represented by the unconformable Adawnib Formation made of proximal carbonate and conglomeratic marine deposits. The change in the type of sedimentation expressed in the facies of the Fars Group, from open to shallow marine carbonate and detritic deposits, was caused by the emergence and erosion of southern Dhofar. Sedimentary conditions were at that time very similar to the present-day environments.

[12] In Jiddat Arkad, the prerift Hadhramaut Group is not exposed. The synrift Ashawq Formation is recognized, but with a thickness of only 100 m. It is directly overlain by the Shuwayr Formation

(200 m thick), which lacks in Dhofar (Figures 2 and 3). It consists of interbedded white bioclastic limestones and debris-flow deposits, which received debris from nearby reefs, and corresponds to a shallower environment than the Mughsayl Formation in Dhofar. The postrift Adawnib Formation is not recognized in Jiddat Arkad where the Warak Formation lies above the Shuwayr Formation and has the same geographical extent and similar facies. It is overlain by the Ghubbarah Formation, which corresponds to the last extensive marine carbonate unit to be deposited in SE Oman. The Ghubbarah Formation transgression advanced from the Indian Ocean about 200 km inland toward the NW. The resulting gulf was very shallow, with paleoenvironments comprising lagoons with reefs. The Shuwayr, Warak, and Ghubbarah formations belong to the same paleogeographical domain open to the Indian Ocean and subjected to extensive subsidence from the Late Oligocene onward. Unlike in Dhofar, the transition between the synrift and the postrift sequences in Jiddat Arkad is not marked by any major unconformity.

[13] In summary, if the prerift history is common to the two regions of Dhofar and Jiddat Arkad, the synrift and postrift evolutions differ significantly. In Dhofar, synrift deposits preserved in grabens are thick and testify to deep marine depositional conditions. By contrast, in Jiddat Arkad, synrift strata are thinner and were deposited in shallow marine conditions. Moreover, while postrift deposits conformably cover synrift strata in Jiddat Arkad, a pronounced unconformity separates the two depositional sequences in Dhofar.

[14] Equivalent rift-related deposits and depositional sequences are described along the conjugate Yemeni and Somali margins of the Gulf of Aden [*Beydoun*, 1970, 1982; *Bosellini*, 1992; *Abbate et al.*, 1993; *Fantozzi*, 1996; *Watchorn et al.*, 1998]. In Yemen, the Shihr Group, equivalent to the Dhofar Group, is early to middle Oligocene (Rupelian-Chattian) in age (34–28 Ma) at the base of the sequence, while the top is middle Burdigalian (18 Ma). An eastward deepening of the synrift deposits is observed from continental to shallow marine (Yemen) and deep marine (Dhofar) conditions.

5. Onshore Deformation of the Oman Passive Margin

[15] The surveyed targets correspond to the main Tertiary deformation zones between Salalah and Ra's Madrakah (Figure 2): from west to east, the Ashawq graben and the area of Salalah, the Hasik graben, the areas of Shuwaymiyah and Sharbithat, and the cape of Ra's Madrakah where ophiolites are exposed. About 790 tectonic joints and striated fault planes were examined in 49 localities scattered along the margin (Table 1). Most fault planes show normal displacements and a minority show strike-slip displacements. On the basis of collection and inversion of fault slip data sets, the orientations of the principal stress axes were determined using computer-aided methods developed by *Angelier* [1984]. In some localities the observed fault slip data sets, too complicated to be explained by a single stress tensor, obviously result from superimposed distinct tectonic events. For such data sets, it is necessary to separate homogeneous subsets identified with A, B, C, or D suffixes (e.g., localities Hasik1, Hasik2, Hasik3, Shuway1, Shuway3, Shuway5, Sharbit2, Madra1, Madra2, and Madra4, in Table 1). The sorting was done in three ways. (1) At sites where all fault planes are similar (e.g., dip-slip normal faults) they can be sorted according to their strikes (locality Shuway1A, B, C). (2) At sites where two different types of fractures are observed (e.g., normal and strike-slip faults), two subsets are distinguished if the fractures are not compatible (locality Madra2A, B). (3) In some exposures, conjugate dip-slip normal faults have been reactivated as oblique slip faults (locality Madra4A, B). In this case, the chronology between the two tectonic stages is obvious.

[16] In localities where fault slip data are scarce or nonexistent, stress inversion is not possible, but the principal axes of deformation can be deduced from the arrangement of tectonic joints [*Hancock*, 1985]. In order to allow a comparison between the stress axes deduced from fault slip data inversion and the deformation axes deduced from joint geometry, we assume that the principal stress axes σ_1, σ_2, and σ_3 are parallel to the shortening, intermediate, and extension axes, respectively.

5.1. Western Margin Segment (Dhofar Region)

5.1.1. Hasik Graben

[17] The Hasik graben strikes parallel to the N75°E regional trend of the Gulf of Aden. It is about 10 km wide and 30 km long, and probably extends seaward in the Kuria Muria bay (Figure 4). It is bounded to the north and south by two normal master faults with a N45°E to N75°E trend. The vertical offset of these boundary faults progressively increases

Table 1. Trend and Dip of Principal Stress Axes Computed From Fault Slip Data[a]

Site	Latitude	Longitude	Number of Faults	Formation	Age	σ_1 Strike, Dip, deg	σ_2 Strike, Dip, deg	σ_3 Strike, Dip, deg	Φ
Hasik1A	17°24.863′	55°15.264′	8	Umm Er Radhuma	Thanetian-Ypresian	127, 73	229, 04	321, 16	0.36
Hasik1B	17°24.863′	55°15.264′	6	Umm Er Radhuma	Thanetian-Ypresian	093, 78	216, 06	307, 10	0.42
Hasik2A	17°24.863′	55°15.264′	5	Umm Er Radhuma	Thanetian-Ypresian	101, 75	247, 13	339, 08	0.37
Hasik2B	17°24.863′	55°15.264′	5	Umm Er Radhuma	Thanetian-Ypresian	012, 72	216, 16	124, 07	0.50
Hasik3A	17°24.385′	55°14.936′	5	Umm Er Radhuma	Thanetian-Ypresian	100, 67	312, 20	218, 11	0.28
Hasik3B	17°24.385′	55°14.936′	6	Umm Er Radhuma	Thanetian-Ypresian	279, 71	022, 04	114, 19	0.50
Hasik3C	17°24.385′	55°14.936′	4	Umm Er Radhuma	Thanetian-Ypresian	068, 72	198, 12	290, 13	0.54
Hasik3D	17°24.385′	55°14.936′	12	Umm Er Radhuma	Thanetian-Ypresian	070, 09	236, 81	340, 02	0.40
Hasik4	17°24.269′	55°14.861′	18	Umm Er Radhuma	Thanetian-Ypresian	088, 21	243, 67	355, 09	0.54
Hasik5	17°26.009′	55°16.270′	4	Umm Er Radhuma	Thanetian-Ypresian	070, 62	252, 28	162, 01	0.70
Shuway1A	17°56.958′	55°39.943′	26	Aydim	Priabonian	105, 83	247, 06	338, 04	0.41
Shuway1B	17°56.958′	55°39.943′	16	Aydim	Priabonian	282, 82	147, 06	056, 06	0.22
Shuway1C	17°56.958′	55°39.943′	22	Aydim	Priabonian	205, 83	107, 01	017, 07	0.39
Shuway1D	17°56.958′	55°39.943′	7	Aydim	Priabonian	042, 74	225, 16	135, 01	0.59
Shuway2	17°56.958′	55°39.943′	15	Aydim	Priabonian	027, 81	239, 08	148, 05	0.46
Shuway3A	17°53.630′	55°43.169′	9	Shuwayr	Oligocene-Early Miocene	278, 86	155, 03	065, 04	0.42
Shuway3B	17°53.630′	55°43.169′	9 joints	Shuwayr	Oligocene-Early Miocene				
Shuway4	17°55.983′	55°42.682′	19 joints	Damman Fm, Uyun Mb	Lutetian-Bartonian				
Shuway5A	17°57.215′	55°39.273′	7	Aydim	Priabonian	169, 80	067, 02	337, 10	0.40
Shuway5B	17°57.215′	55°39.273′	8	Aydim	Priabonian	127, 74	280, 14	011, 07	0.39
Sharbit1	17°57.035′	56°15.986	11 joints	Warak	Early-Middle Miocene				
Sharbit2A	17°57.146′	56°15.612′	12 joints	Warak	Early-Middle Miocene				
Sharbit2B	17°57.146′	56°15.612′	18 joints	Warak	Early-Middle Miocene				
Sharbit2C	17°57.146′	56°15.612′	6 joints	Warak	Early-Middle Miocene				
Sharbit3	17°56.590′	56°10.482′	10	Shuwayr	Oligocene-Early Miocene	152, 73	282, 11	015, 13	0.29
Sharbit4	17°55.903′	56°08.702′	7	Shuwayr	Oligocene-Early Miocene	019, 77	234, 11	143, 07	0.49
Madrak1A	18°58.597′	57°47.142′	11	Warak	Early-Middle Miocene	032, 57	216, 33	125, 02	0.44
Madrak1B	18°58.597′	57°47.142′	12	Warak	Early-Middle Miocene	255, 06	137, 78	346, 11	0.70
Madrak2A	18°58.221′	57°48.169′	21	Shuwayr	Oligocene-Early Miocene	023, 79	238, 09	147, 06	0.26
Madrak2B	18°58.221′	57°48.169′	22	Shuwayr	Oligocene-Early Miocene	211, 03	084, 86	301.03	0.76
Madrak3	18°59.288′	57°47.898′	16 joints	Shuwayr	Oligocene-Early Miocene				
Madrak4A	18°58.990′	57°48.034′	22	Shuwayr	Oligocene-Early Miocene	201, 85	068, 04	338, 04	0.38
Madrak4B	18°58.990′	57°48.034′	5	Shuwayr	Oligocene-Early Miocene	116, 76	194, 14	024, 00	0.44
Madrak4C	18°58.990′	57°48.034′	10	Shuwayr	Oligocene-Early Miocene	257, 02	357, 81	167, 09	0.50
Madrak5	18°58.823′	57°48.107′	4	Shuwayr	Oligocene-Early Miocene	315, 15	089, 69	221, 15	0.57
Madrak6	19°02.495′	57°48.647′	5	Shuwayr	Oligocene-Early Miocene	202, 59	022, 32	292, 00	0.62
Sawqirah	18°10.681′	56°32.297′	6	Shuwayr	Oligocene-Early Miocene	312, 07	102, 82	222, 04	0.49
Hadbin1	17°14.401	55°13.302	18	Umm Er Radhuma	Thanetian-Ypresian	111, 86	341, 02	251, 03	0.37
Hadbin2	17°14.401	55°13.302	6	Umm Er Radhuma	Thanetian-Ypresian	358, 81	124, 05	215, 07	0.24
Salala1	16°52.957	53°46.954	12	Mughsayl	Oligocene-Early Miocene	61, 82	307, 03	216, 07	0.33
Salala2	16°49.042	53°37.512	12	Ashawq Fm, Nakhlit Mb	Rupelian-Chattian	71, 87	240, 03	330, 01	0.39
Salala3	16°52.653	53°43.282	8	Ashawq Fm, Nakhlit Mb	Rupelian-Chattian	58, 35	267, 51	159, 14	0.41

Table 1. (continued)

Site	Latitude	Longitude	Number of Faults	Formation	Age	σ_1 Strike, Dip, deg	σ_2 Strike, Dip, deg	σ_3 Strike, Dip, deg	Φ
Salala4	16°52.138	53°46.029	9	Mughsayl	Oligocene-Early Miocene	191, 70	291, 04	23, 19	0.03
Salala6	17°01.891	54°34.535	10 joints	Umm Er Radhuma	Thanetian-Ypresian				
Salala7	17°01.879	54°36.778	11	Dalqut Fm, Sarfait Mb	Cenomanian-Turonian	134, 88	294, 02	24, 01	0.49
Salala8A	17°04.387	54°26.994	11	Dammam Fm, Qara Mb	Lutetian-Bartonian	7, 78	274, 01	184, 11	0.38
Salala8B	17°04.387	54°26.994	5 joints	Dammam Fm, Qara Mb	Lutetian-Bartonian				
Salala8C	17°04.387	54°26.994	8	Dammam Fm, Qara Mb	Lutetian-Bartonian	72, 17	289, 68	165, 12	0.56
Salala9	17°04.846	54°24.979	5	Umm Er Radhuma	Thanetian-Ypresian	101, 78	248, 10	339, 07	0.38
Salala10A	17°13.428	54°23.986	11 joints	Rus	Cuisian				
Salala10B	17°13.428	54°23.986	6 joints	Rus	Cuisian				
Salala13A	17°08.390	54°08.020	10	Umm Er Radhuma	Thanetian-Ypresian	290, 73	65, 12	158, 11	0.31
Salala13B	17°08.390	54°08.020	7	Umm Er Radhuma	Thanetian-Ypresian	138, 81	347, 08	257, 04	0.26
Salala15A	17°08.431	54°08.058	2, 4 joints	Umm Er Radhuma	Thanetian-Ypresian				
Salala15B	17°08.431	54°08.058	3	Umm Er Radhuma	Thanetian-Ypresian				
Salala18	16°44.887	53°25.805	14	Ashawq Fm, Shizar Mb	Rupelian	225, 69	78, 17	345, 10	0.24
Salala19A	16°49.924	53°20.260	8 joints	Rus	Cuisian				
Salala19B	16°49.924	53°20.260	5 joints	Rus	Cuisian				
Salala20	16°48.280	53°32.577	14	Umm Er Radhuma	Thanetian-Ypresian	167, 81	61, 03	331, 08	0.36
Salala21	16°49.874	53°39.672	14	Ashawq Fm, Nakhlit Mb	Rupelian-Chattian	195, 81	54, 07	323, 05	0.36
Salala22	16°55.304	53°44.326	18	Mughsayl	Oligocene-Early Miocene	354, 85	247, 01	157, 05	0.44
Salala31	16°55.268	53°22.920	9	Ashawq Fm, Nakhlit Mb	Rupelian-Chattian	24, 77	219, 12	128, 03	0.42
Salala32	16°49.207	53°37.484	5	Ashawq Fm, Nakhlit Mb	Rupelian-Chattian	32, 81	229, 09	139, 03	0.47
Salala33	16°49.796	53°39.756	21	Ashawq Fm, Nakhlit Mb	Rupelian-Chattian	20, 89	242, 01	152, 01	0.36
Salala34	16°52.300	53°43.400	4	Mughsayl	Oligocene-Early Miocene	218, 74	84, 11	352, 12	0.72
Salala35A	16°54.529	53°49.342	1, 18 joints	Mughsayl	Oligocene-Early Miocene				
Salala35B	16°54.529	53°49.342	21 joints	Mughsayl	Oligocene-Early Miocene				
Salala35C	16°54.529	53°49.342	1, 14 joints	Mughsayl	Oligocene-Early Miocene				
Salala36	16°53.000	53°47.200	3, 5 joints	Mughsayl	Oligocene-Early Miocene				
Salala37	16°53.300	53°46.800	12	Mughsayl	Oligocene-Early Miocene	130, 79	262, 08	353, 08	0.37
Salala38	16°53.400	53°49.300	3, 7 joints	Mughsayl	Oligocene-Early Miocene				
Salala39	16°52.957	53°46.954	4	Mughsayl	Oligocene-Early Miocene	1, 78	112, 04	202, 11	0.49
Salala40	16°54.500	53°49.400	3, 10 joints	Mughsayl	Oligocene-Early Miocene				
Salala41	16°56.300	53°46.500	7	Mughsayl	Oligocene-Early Miocene	54, 82	293, 04	203, 07	0.29

[a] Here σ_1, σ_2, and σ_3 are maximum, intermediate, and minimum principal stress axes. Φ is the ratio $(\sigma_2 - \sigma_3)/(\sigma_1 - \sigma_3)$. Fm is formation, Mb is member.

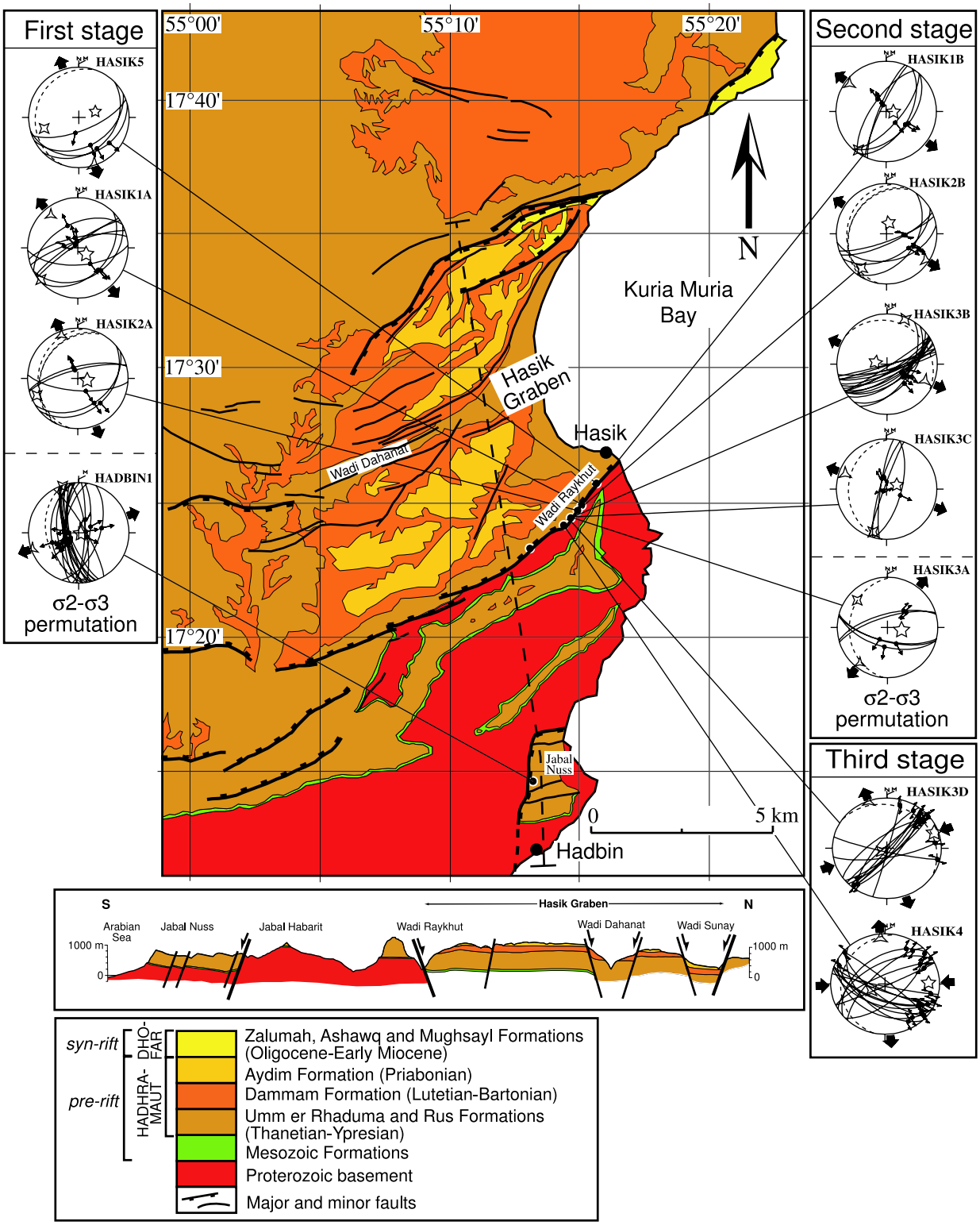

Figure 4. Stress fields recorded in the Eocene Umm Er Radhuma Formation in the Hasik graben. Two directions of extension are inferred from fault slip data (equal-area lower hemisphere projection). The N150°E–N160°E direction (stage 1) and the N30°E–N40°E direction (stage 2) are representative of the regional deformation. The N110°E–N130°E and N70°E directions reflect local permutations between the σ_2 and σ_3 stress axes. An ENE-WSW direction of compression is deduced from strike-slip faults (stage 3). Stars in stereonets correspond to the principal stress axes: σ_1 (five branches), σ_2 (four branches), and σ_3 (three branches). Arrows show the trend of the horizontal principal stresses computed (solid arrows) or inferred (open arrows) from fracture analysis. Dashed line is for the bedding plane.

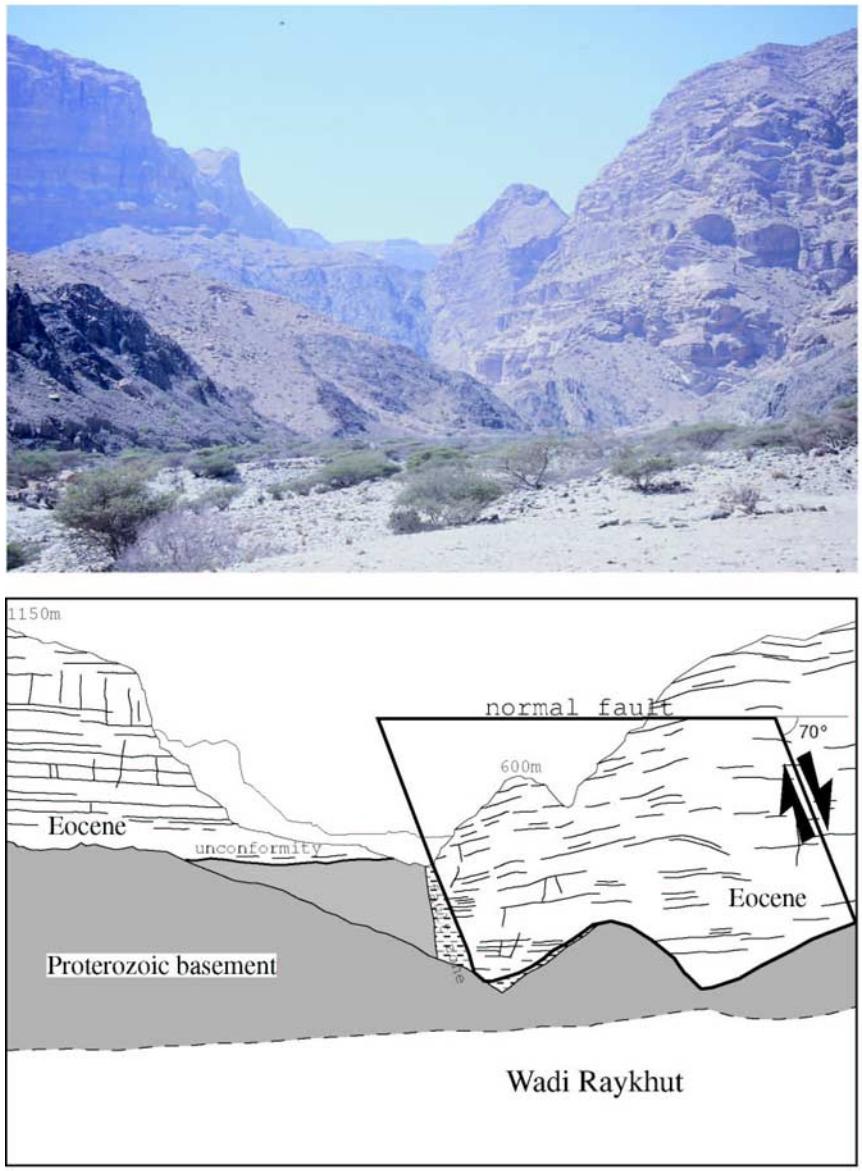

Figure 5. Major normal fault of the passive margin in the wadi Raykhut, Hasik graben (view toward the west). The fault strikes N50°E and dips toward the north of ~70°, and its vertical offset exceeds 500 m (see cross section in Figure 4).

toward the east, so that the graben presents an axial dip of a few degrees toward the east. The southern bounding master fault of wadi Raykhut brings into contact the Proterozoic basement with the middle part of the Umm Er Radhuma Formation (Figures 4 and 5). The fault can be followed over several kilometers along the wadi Raykhut and can locally be observed in detail. It dips 60°–70° toward the NW (Figure 5). The fault zone, which separates the basement from the Eocene limestones, is several meters wide. The vertical offset of the fault reaches 500–600 m (cross section in Figure 4). In the graben, a network of plurikilometer-scale, steeply dipping normal faults trending ENE-WSW cuts the horizontal Eocene series. The vertical offset of the northern bounding master fault reaches 800 m [*Platel et al.*, 1992c]. South of the Hasik graben, Jabal Nuss is a large tectonic block tilted toward the northwest, bounded by a major normal fault trending N20°E to the west and N80°E to the north. Its vertical offset reaches 1000 m to the north [*Platel and Roger*, 1989].

[18] In the Wadi Raykhut, minor faults have been measured in the vicinity of the main fault in the Umm Er Radhuma Formation. Two sets of normal

faults can be distinguished: faults parallel to the main fault and trending about N70°E (from N50°E to N90°E; sites Hasik1A, 2A, 2B, 3A, 3B, 5), and faults trending from about N30°E (from N-S to N40°E; sites Hasik1B, 3C). The N30°E trending conjugate dip-slip normal faults document a N110°E–N130°E extension. The N70°E trending faults are either dip-slip normal faults indicating a N150°E–N160°E extension (sites Hasik1A, 2A, 5), or oblique normal faults indicating a N110°E–N130°E extension like the N30°E trending faults (sites Hasik2B, 3B). These observations allow us to conclude to the succession of two stages of extension: an older, N150°E–N160°E extensional phase causing the observed N70°E faulting and a younger, N110°E–N130°E extensional phase responsible for the observed N30°E faulting and the reactivation of the N70°E faults as oblique normal faults. Moreover, a set of conjugate normal faults pertaining to the N70°E trending faults has been reactivated as oblique slip normal faults and indicates a N30°E–N40°E extensional episode (site Hasik3A). This extension again postdates the earlier N150°E–N160°E extension. The two late extensions, which are nearly orthogonal (N110°E–N130°E and N30°E–N40°E), could be attributed to two different diachronous stress fields, but we interpret them here in terms of permutations between the two principal horizontal σ_2 and σ_3 axes within a unique extensional stress field [e.g., *Bergerat et al.*, 1998; *Fournier et al.*, 2001a]. In the same way, the N70°E trending extension documented by a set of conjugate normal faults trending approximately N-S (from N20°W to N10°E; site Hadbin1) in the Jabal Nuss near Hadbin, is considered to pertain to the same stress field as the N150°E–N160°E extensional episode and to reflect permutations between the σ_2 and σ_3 stress axes.

[19] In summary, four directions of extension pertaining to two stress fields with local permutations between σ_2 and σ_3 are documented. The N150°E–N160°E direction, perpendicular to the mean orientation of the Gulf of Aden, and the N20°E–N40°E direction, parallel to the direction of divergence between the Arabian and Somalia plates, are recorded along the entire margin from Yemen [*Huchon and Khanbari*, 2003] to Dhofar [*Lepvrier et al.*, 2002]. They are therefore representative of the regional deformation. The perpendicular N70°E and N110°E–N130°E directions may simply reflect local permutations between σ_2 and σ_3.

[20] Finally, two sites in the Umm Er Radhuma Formation display conjugate sets of strike-slip faults, right-lateral faults trending NE-SW and left-lateral faults trending E-W to SE-NW (sites Hasik3D, Hasik4). Stress inversion gives $\sigma_{Hmax} = \sigma_1$ trending N70°E to N90°E. Where a chronology can be observed on fault planes, strike-slip motions are always posterior to normal motions. The WSW-ENE compressional episode documented by the strike-slip faults therefore postdated the extensional episodes described above.

5.1.2. Ashawq Graben and Salalah Area

[21] The prominent structure of the Salalah region is the Ashawq graben where synrift and postrift series are widely exposed (Figure 6). This graben is bounded to the south by the coastal horst of Jabal Al Qamar, which is in turns bordered to the southwest by a zone of seaward dipping fault blocks stepping down into the sea. The Ashawq graben is approximately 20 km wide and is bounded by two normal master faults of opposite dip. The northern bounding fault is composed of three segments trending, from west to east, N110°E, N70°E, and again N110°E. The vertical offset of the fault exceeds 1500 m to the north of Salalah [*Platel and Roger*, 1989]. The southern bounding fault trends N75°E and its throw is estimated to be ca. 500 m. In its western part, the Ashawq graben is intensely dissected by a set of NE trending normal faults mostly dipping toward the southeast. They branch to the north on the N110°E bounding fault. The horsetail geometry of the splay indicates a left-lateral component of slip along the northern bounding fault.

[22] Minor faults have been measured mainly in the Ashawq graben and along the fault escarpment bordering the Salalah plain (Figure 6). Two sets of dip-slip conjugate normal faults can be distinguished, one set trending between N45°E and N90°E and indicating a N150°E–N160°E extension, and the second set trending ca. N110°E and indicating a N20°E–N30°E extension. A set of N160°E to N-S trending extensional joints has also been measured, which indicates a direction of extension N70°E to E-W, perpendicular to the

Figure 6. Stress fields recorded in the Eocene to Early Miocene formations of the Ashawq graben and Salalah region. Two directions of extension are inferred from fault slip data: a N150°E–N160°E direction (stage 1) and a N20°E–N30°E direction (stage 2). The sites Salala1 to Salala22 are recomputed from *Lepvrier et al.* [2002].

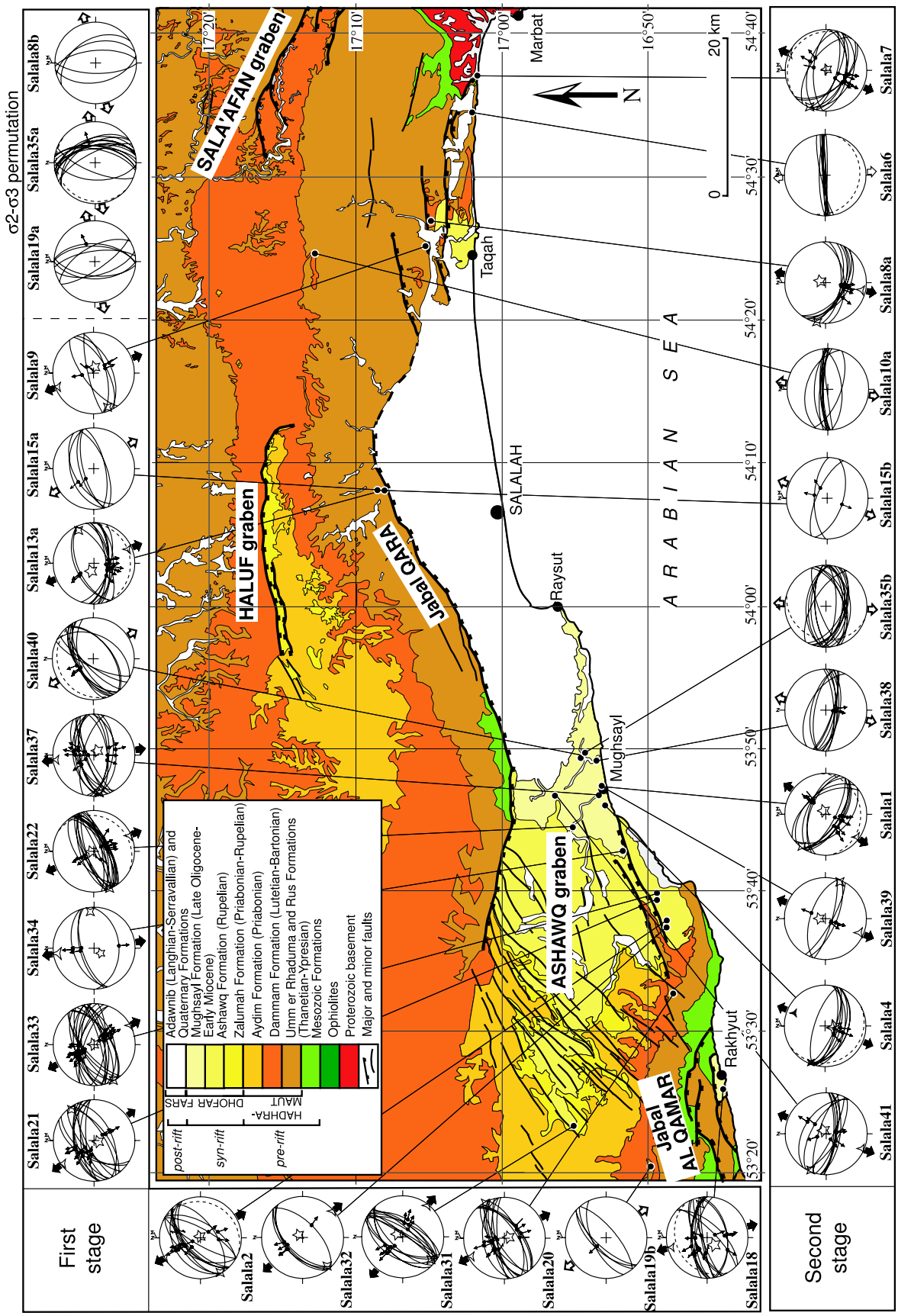
First stage
Second stage
σ2-σ3 permutation
Salala21
Salala33
Salala34
Salala22
Salala37
Salala40
Salala13a
Salala15a
Salala9
Salala19a
Salala35a
Salala8b
Salala2
Salala32
Salala31
Salala20
Salala19b
Salala18
Salala41
Salala4
Salala39
Salala1
Salala38
Salala35b
Salala15b
Salala10a
Salala8a
Salala6
Salala7
SALA'AFAN graben
HALUF graben
Jabal QARA
ASHAWQ graben
Jabal AL QAMAR
ARABIAN SEA
SALALAH
Taqah
Marbat
Raysut
Mughsayl
Rakhyut
17°20'
17°10'
17°00'
16°50'
54°40'
54°30'
54°20'
54°10'
54°00'
53°50'
53°40'
53°30'
53°20'
0
20 km
N
Adawnib (Langhian-Serravallian) and Quaternary Formations
Mughsayl Formation (Late Oligocene-Early Miocene)
Ashawq Formation (Rupelian)
Zalumah Formation (Priabonian-Rupelian)
Aydim Formation (Priabonian)
Dammam Formation (Lutetian-Bartonian)
Umm er Rhaduma and Rus Formations (Thanetian-Ypresian)
Mesozoic Formations
Ophiolites
Proterozoic basement
Major and minor faults
post-rift
syn-rift
pre-rift
DHOFAR FARS
HADHRA-MAUT

Figure 6

dominant N150°E–N160°E direction of extension (sites Salala8b, 19a, 35a). This minor extension may reflect permutations between σ_2 and σ_3.

[23] The two main directions of extension are recorded through the entire Tertiary sediment pile up to the Late Oligocene-Early Miocene Mughsayl Formation. They generally cannot be observed in the same site (except in Salala15) and no direct crosscutting relationships can be observed. Hence it is not possible to establish a relative succession between these two episodes in the Ashawq graben. The chronology proposed in Figure 6 is inferred from the chronologies determined in the Hasik graben and Ra's Madrakah areas.

5.2. Eastern Margin Segment (Jiddat Arkad Region)

5.2.1. Shuwaymiyah and Sharbithat

[24] The Jabal Qarabiyan in the area of Shuwaymiyah separates a western domain, dominated by the prerift deposits of the Hadhramaut Group, and an eastern domain where the postrift Fars Group prevails indicating the existence of an extensive basin subsiding from the Late Oligocene to the Middle Miocene (Figures 2 and 7). The vertical throw of the N30°E trending normal fault of Jabal Qarabiyan is several hundred meters near Shuwaymiyah (cross section in Figure 7). We did not find any field evidence of strike-slip motion along the Jabal Qarabiyan fault, which was apparently not reactivated during the spreading phase.

[25] In the area of Sharbithat, fault scarps of kilometric extent are expressed in the coastal topography. They are found in the Oligocene-Early Miocene limestone of the Shuwayr Formation. They trend approximately E-W, face predominantly southward, and their trace in map view is concave toward the sea (Figure 7). The height of the scarps is several tens of meters. They define a step-wise structure with the Shuwayr Formation downthrown southward. *Platel et al.* [1992b] described evidence of synsedimentary tectonics and dated the displacements along the faults to the Late Oligocene or earliest Miocene. A less well-documented system of N-S normal faults is interpreted by *Platel et al.* [1992b] as bounding a paleocanyon filled with deposits of the Warak Formation (Figure 7). However, this N-S direction is not represented among the outcrop-scale faults measured in the field.

[26] In the Shuwaymiyah-Sharbithat area, all fault sets provide vertical σ_1 axes after inversion (Figure 7 and Table 1). Three directions of extension have been found. A set of conjugate normal faults trending from N50°E to N80°E (sites Shuway1A, 1D, 2, 4, 5A, Sharbit4) document a N150°E–N160°E extension. Another series of conjugate normal faults indicates a perpendicular N60°E–N70°E direction of extension (sites Shuway1B, 3A, Sharbit2A), which could reflect permutations of the horizontal principal stress axes. A group of conjugate normal faults and extensional joints trending from E-W to N120°E documents a N-S to N20°E extension (sites Shuway1C, 3B, 5B, Sharbit1, 2B, 3). These observations allow us to conclude to the existence of at least two stages of extension: a N150°E–N160°E extension at the origin of the N70°E faulting and possibly the N150°E faulting in response of stress permutations, and a N-S to N20°E extension responsible for the E-W to N120°E faulting.

[27] We did not observe any chronology in the field between the two stages of extension. The chronology presented in Figure 7 refers to chronologies inferred in the Hasik graben and Ra's Madrakah areas. The curved normal faults of kilometric-scale in the area of Sharbithat may equally pertain to the N70°E trending fault group or to the E-W to N120°E trending fault group. One cannot rule out that they document a unique, roughly N-S extension (i.e., between N30°W and N20°E) rather than two diachronous extensional stress fields.

5.2.2. Ra's Madrakah

[28] The ophiolites of Ra's Madrakah were formed during the latest Jurassic and emplaced along the Owen transform margin during latest Maastrichtian to earliest Paleocene times [*Gnos et al.*, 1997; *Peters and Mercolli*, 1998]. They are unconformably covered by the Oligocene to Middle Miocene limestone of the Shuwayr and Warak formations (Figure 8). Steeply dipping normal faults trending N-S to N30°E cut these formations and the underlying ophiolites.

[29] Two groups of conjugate normal faults have been measured in the limestone of the Shuwayr Formation (Figure 8): faults trending N50°E to N90°E indicates a N150°E–N160°E direction of extension (sites Madrak2A, 3, 4A) and faults trending N10°E–N30°E document a N110°E–N120°E direction of extension (sites Madrak1A, 6). At the locality Madrak4B, NE-SW trending conjugate normal faults were reactivated as oblique normal faults defining a N20°E extension. The fault reactivation demonstrates the succession of two

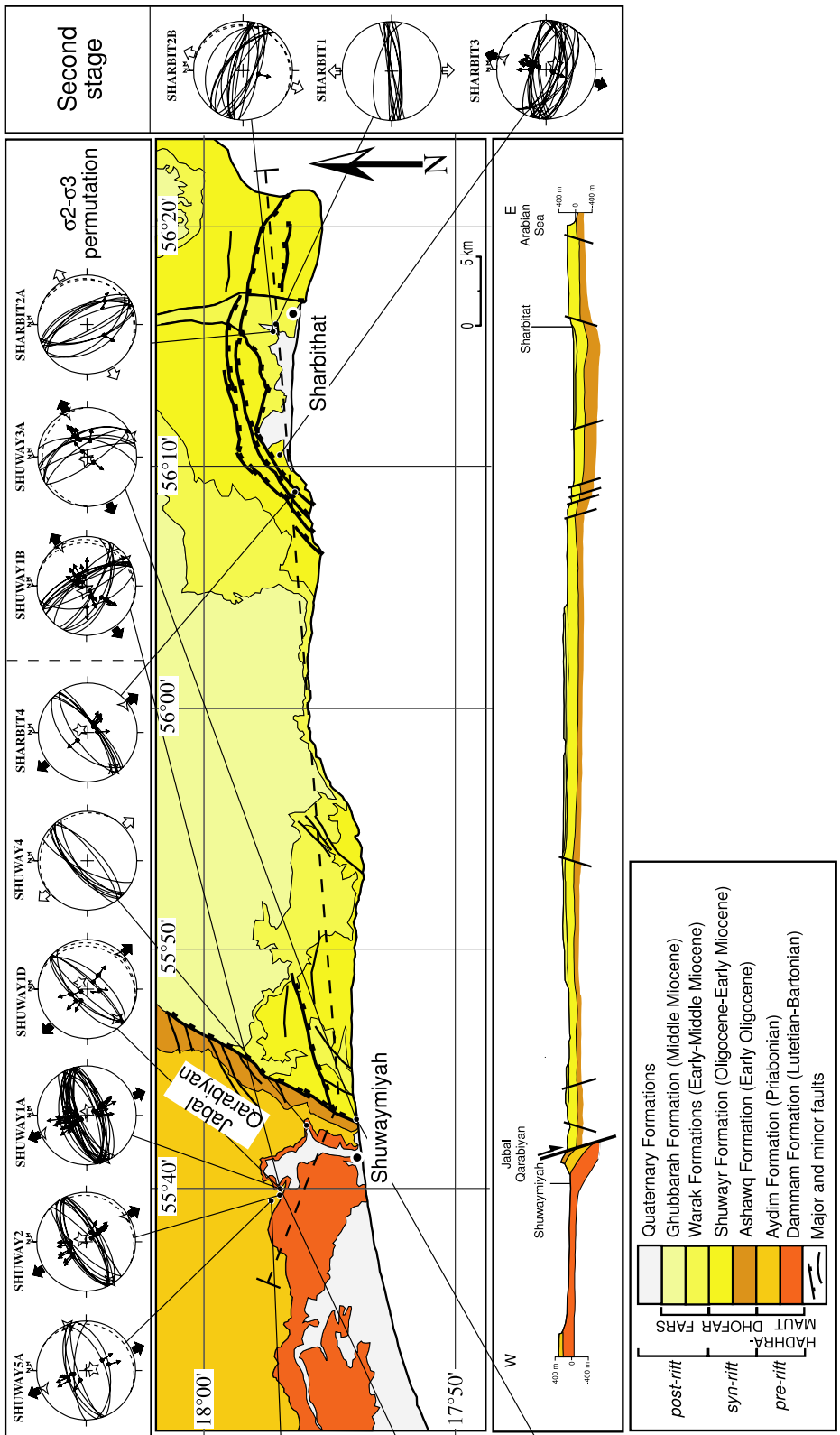

Figure 7. Stress fields recorded in the Eocene to Early Miocene formations of the Shuwaymiyah and Sharbithat areas. Two main directions of extension representative of the regional deformation are documented by fault slip data: a N150°E–N160°E direction and a N-S to N25°E direction. A direction of extension N60°E perpendicular to the N160°E one is considered to reflect local permutation between the σ_2 and σ_3 stress axes.

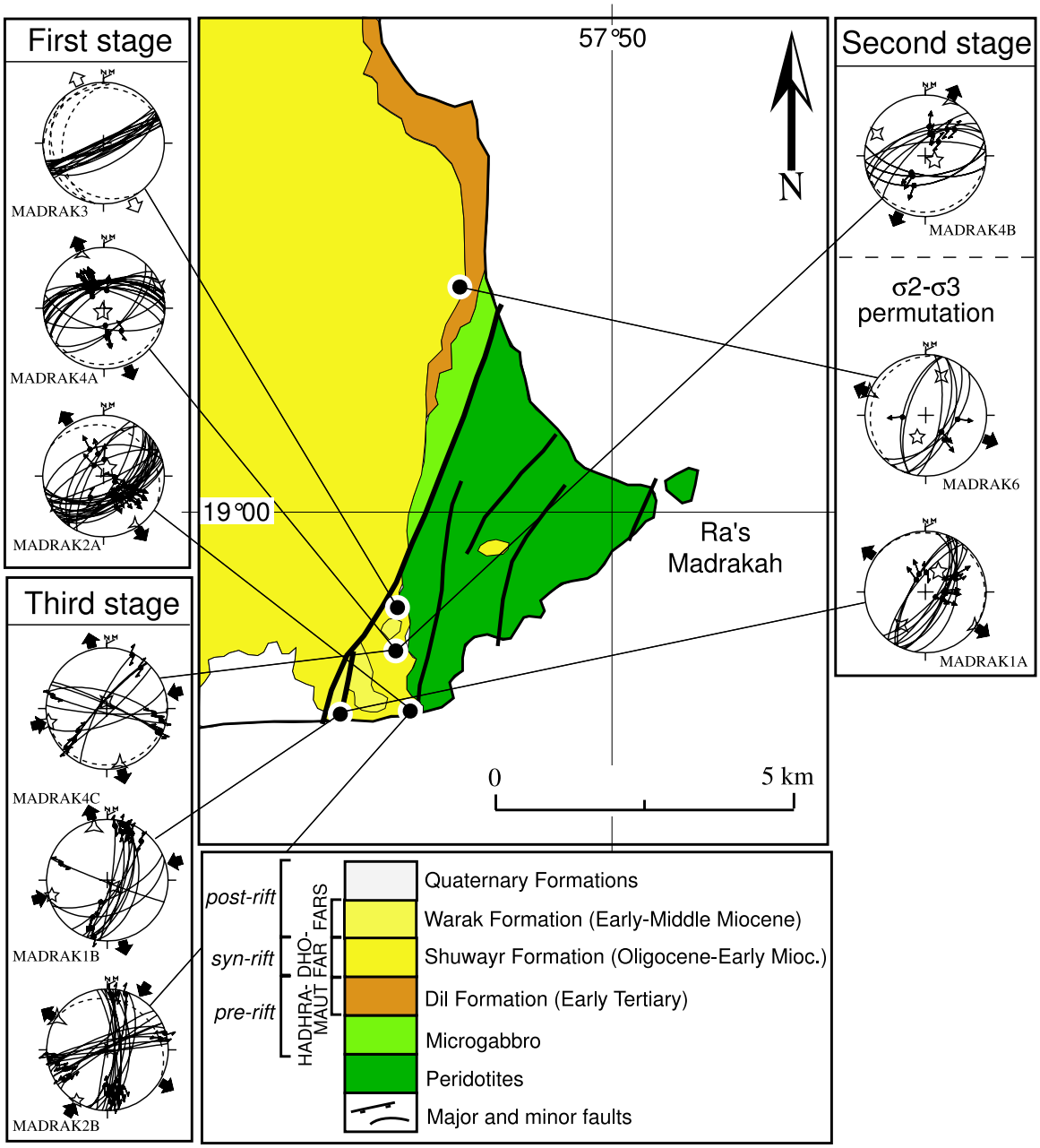

Figure 8. Stress fields recorded in the Oligocene to Early-Middle Miocene Shuwayr and Warak formations of Ra's Madrakah. Two main directions of extension are documented: N150°E–N160°E and N20°E–N30°E. A N110°E–N120°E direction of extension perpendicular to the N20°E–N30°E is interpreted in terms of permutations between σ_2 and σ_3. A late NE-SW direction of compression is documented by conjugate strike-slip faults.

episodes of extension: an older N150°E–N160°E extension at the origin of the N50°E to N90°E faulting and a younger N20°E extension responsible for the reactivation of the ENE-WSW normal faults. The N110°E–N120°E direction of extension, perpendicular to the late extension, can be again interpreted in terms of stress permutations. This interpretation is consistent with the fact that the N30°E faults cut the Warak Formation at site Madrak1A (Figure 8) and seem to be younger than the ENE-WSW faults, which have been only observed in the older Shuwayr Formation.

[30] Finally, three sites in the Shuwayr and Warak formations display conjugate sets of strike-slip faults (sites Madrak1B, 2B, 4C) and document an intermediate-type regional stress field with $\sigma_{Hmax} = \sigma_1$ trending NE-SW. Crosscutting structures show

that strike-slip motions are posterior to normal motions.

5.3. Regional Synthesis: Two Distinct Phases of Extension or Two Coexisting Extensional Stress Fields?

[31] Figure 9 provides a synthesis of the outcrop-scale deformation of the northeastern margin of the Gulf of Aden since the Eocene. We identify three main phases of deformation with the following relative chronology from the oldest to the youngest, (1) a N150°E–N160°E extension, (2) a N-S to N30°E extension, and (3) a strike-slip event corresponding to NE-SW compression and NW-SE extension. The two extensions are documented everywhere along the margin, whereas the strike-slip regime has not been observed in the areas of Shuwaymiyah and Sharbithat. Two additional directions of extension perpendicular to the predominant directions of extension are also recognized. They are interpreted in terms of stress permutations between σ_2 and σ_3 within a unique stress field. The strike-slip event unambiguously postdates the extensional episodes.

[32] The two main directions of extension are recorded in the entire Tertiary sedimentary pile, from the Eocene Umm Er Radhuma Formation up to the Oligocene-Early Miocene Mughsayl and Shuwayr formations. The two extensions correspond to a synsedimentary activity during the deposition of the Mughsayl and Shuwayr formations in Late Oligocene-Early Miocene time [*Lepvrier et al.*, 2002; *Platel et al.*, 1992b]. However, it cannot be excluded that these extensions were already active before this time. The two directions coexist in some localities (sites Salala15A and 15B, Shuway1A and 1C, Madrak4A and 4B), but no crosscutting structure could be observed. The relative chronology between the two phases is deduced from the observation, in several localities, of conjugate normal faults initially formed during the N150°E–N160°E extensional episode, and reactivated as oblique normal faults during the N-S to N30°E extensional episode (Madrak4A, 4B) or its N110°E–N120°E permutation (Hasik2A, 2B, Hasik3A, 3B). Hence the two directions of extension could be considered as distinct events of probably Late Oligocene to Early Miocene age, with the N150°E–N160°E extension preceding the N-S to N30°E extension. They might, however, also constitute a continuous process with progressive reorientation of the directions of extension through time, as suggested by the existence of numerous curved normal faults.

[33] The normal fault pattern was studied in several places along the margins of the Gulf of Aden, including Somalia [*Fantozzi*, 1996] and Yemen [*Huchon and Khanbari*, 2003]. As in Oman, two N20°E and N160°E directions of extension were identified along the northern margin of the Gulf of Aden in Yemen [*Huchon and Khanbari*, 2003]. *Huchon and Khanbari* [2003] suggest that the N20°E extension predates the N160°E one and conclude to the counterclockwise rotation of the synrift stress field. However, some of their data also suggest a reverse chronology (sites SHIR28 and MAS34 in their Figure 6; site HAUF16 in their Figure 7). Our data in Dhofar and Jiddat Arkad contradict the chronology of the extensional episodes in Yemen and rather suggest that the N160°E extension predates the N20°E one. Two opposite chronologies have therefore been inferred on the northern margin of Gulf of Aden, but nowhere has it been possible to establish them unambiguously. The attribution of two different ages to the two different stress fields is inconsistent with the data. This could signify that both extension directions coexisted during the rifting. The coexistence of two stress fields has sometimes been observed in past and present-day deformation [e.g., *Eyal*, 1996; *Garcia et al.*, 2002] and is interpreted in terms of a second-order local stress field superimposed on a first-order remote regional field [*Zoback*, 1992]. The second-order local stress field could reflect a local perturbation of the first-order stress field caused by a heterogeneity in the lithosphere.

6. Synthesis of Onshore and Offshore Data

[34] Figure 10 shows a synthetic structural map of the offshore and onshore domains of the passive margin. The offshore structural map has been obtained from the analysis of swath bathymetry and seismic reflection profiles [*d'Acremont*, 2002]. These data show that the Socotra fracture zone

Figure 9. Synthesis of on-land deformation on the northeastern margin of the Gulf of Aden. Three successive episodes of deformation are recognized: a N150°E–N160°E extension, a N-S to N30°E extension, and a strike-slip deformation with σ_1 trending NE-SW. Perpendicular directions of extension reflect permutations between the σ_2 and σ_3 stress axes.

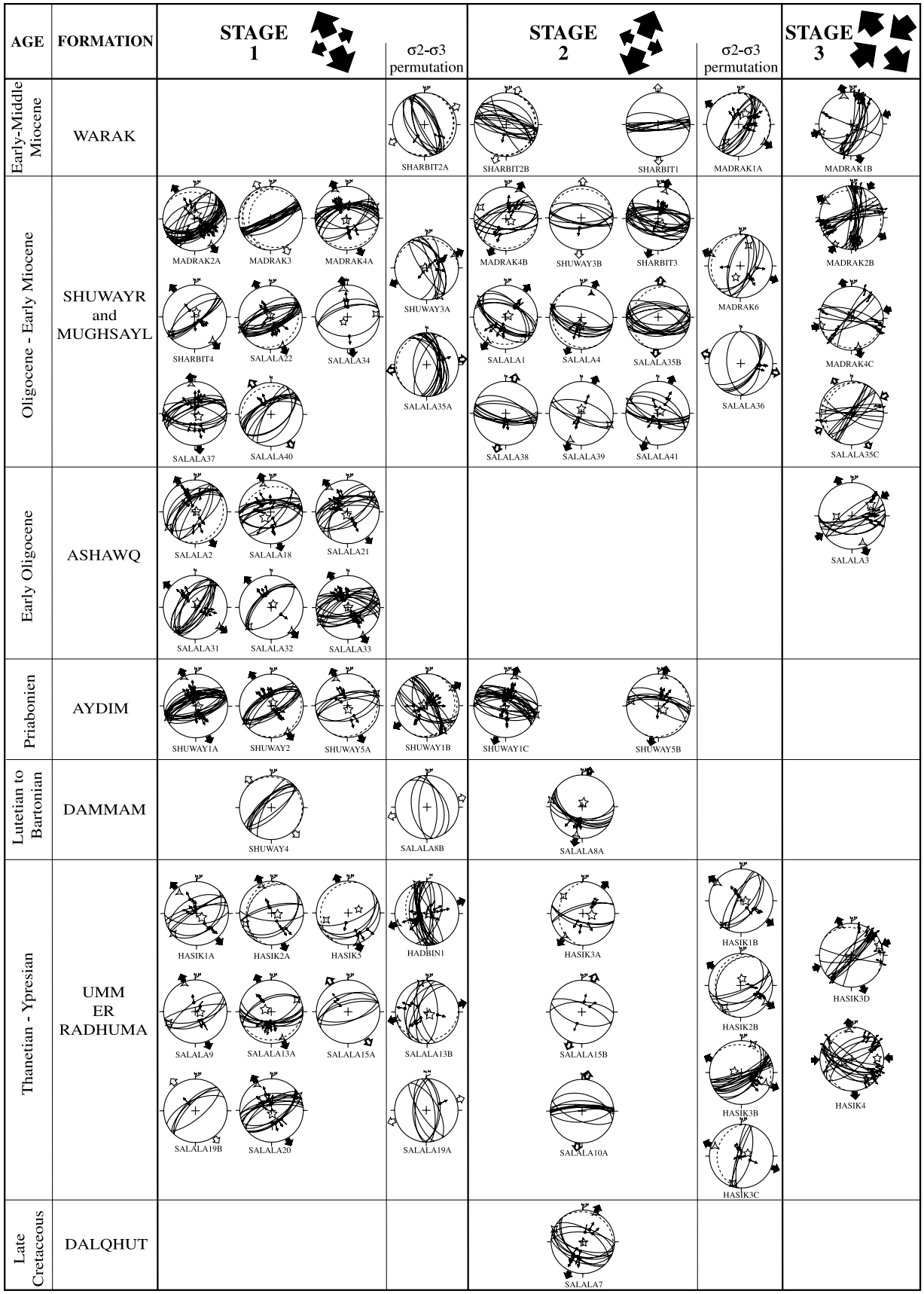
AGE
FORMATION
STAGE 1
σ2-σ3 permutation
STAGE 2
σ2-σ3 permutation
STAGE 3
Early-Middle Miocene
WARAK
SHARBIT2A
SHARBIT2B
SHARBIT1
MADRAK1A
MADRAK1B
Oligocene - Early Miocene
SHUWAYR and MUGHSAYL
MADRAK2A
MADRAK3
MADRAK4A
SHUWAY3A
MADRAK4B
SHUWAY3B
SHARBIT3
MADRAK6
MADRAK2B
SHARBIT4
SALALA22
SALALA34
SALALA35A
SALALA1
SALALA4
SALALA35B
MADRAK4C
SALALA37
SALALA40
SALALA38
SALALA39
SALALA41
SALALA36
SALALA35C
Early Oligocene
ASHAWQ
SALALA2
SALALA18
SALALA21
SALALA3
SALALA31
SALALA32
SALALA33
Priabonien
AYDIM
SHUWAY1A
SHUWAY2
SHUWAY5A
SHUWAY1B
SHUWAY1C
SHUWAY5B
Lutetian to Bartonian
DAMMAM
SHUWAY4
SALALA8B
SALALA8A
Thanetian - Ypresian
UMM ER RADHUMA
HASIK1A
HASIK2A
HASIK5
HADBIN1
HASIK3A
HASIK1B
HASIK3D
SALALA9
SALALA13A
SALALA15A
SALALA13B
SALALA15B
HASIK2B
HASIK4
SALALA19B
SALALA20
SALALA19A
SALALA10A
HASIK3B
HASIK3C
Late Cretaceous
DALQHUT
SALALA7

Figure 9

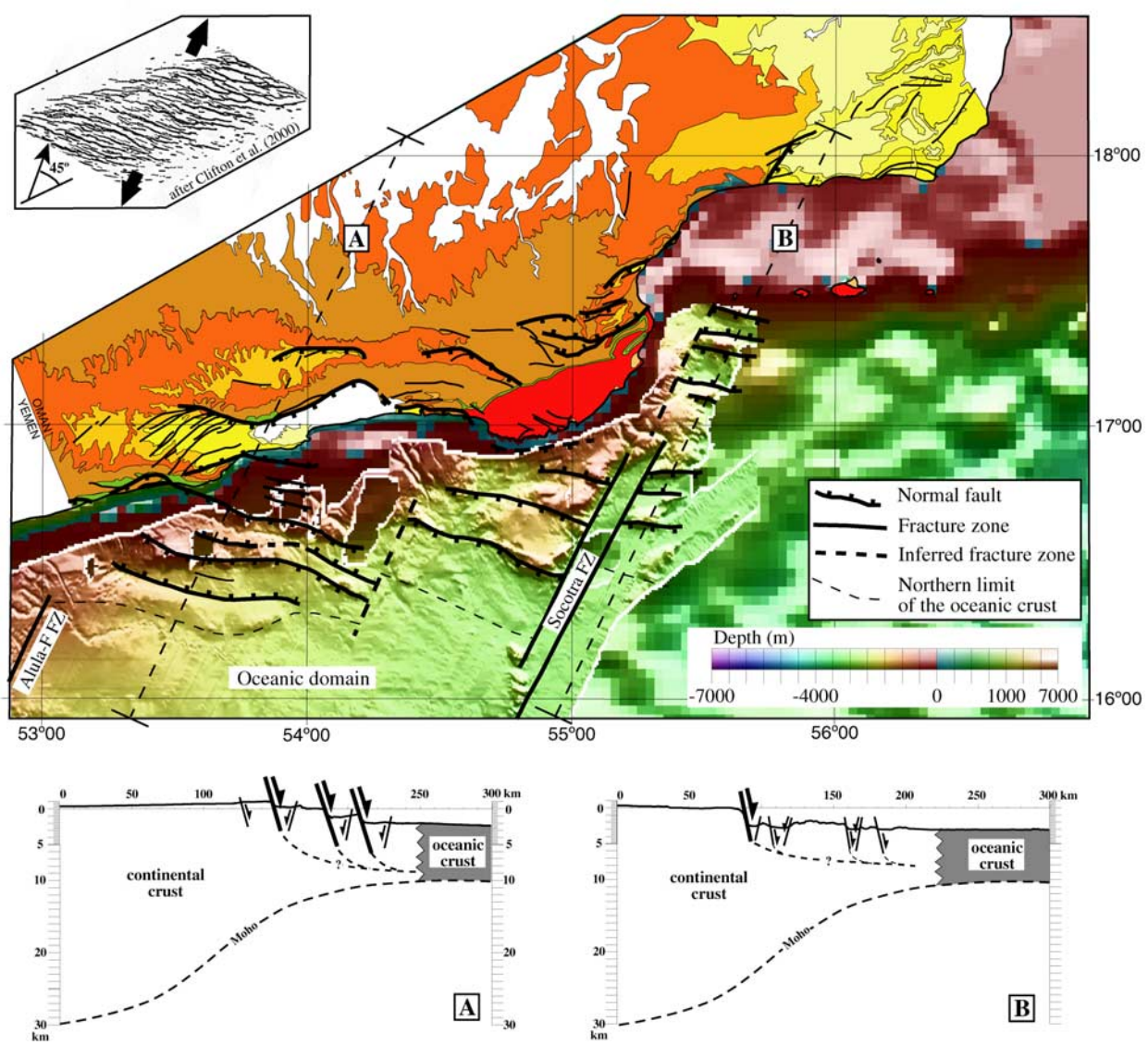

Figure 10. Structural map of the northeastern passive margin of the Gulf of Aden established from swath-bathymetric and seismic data offshore [*d'Acremont*, 2002] and geological maps onshore (same legend as Figure 2). In the offshore domain the bathymetric map from multibeam soundings recorded during the Encens-Sheba cruise [*Leroy et al.*, 2004] is superimposed on the bathymetric map of *Sandwell and Smith* [1997]. The normal faults of the lower margin (offshore) are linear and trend N110°E–120°E, while the normal faults of the upper margin (onshore) are sigmoidal with a mean N75°E trend. Inserts show fault pattern for experimental clay model of oblique rifting, with a rifting obliquity of 45° as in the Gulf of Aden [after *Clifton et al.*, 2000]. Plots A and B are interpretative crustal-scale sections of the western and eastern segments of the Oman passive margin. Major faults (thick lines) correspond to the main topographic escarpments of the margins. Geometries of faults at depth and Moho are speculative.

can be followed across the lower part of the continental margin and abuts against the continental platform at its northern extremity. Two interpretative crustal-scale cross sections of the margin on either side of the fracture zone illustrate the contrasted style of faulting of the margin segments. The western margin is shorter than the eastern one, is characterized by an uplifted shoulder, and is controlled by three major normal faults which correspond to the main escarpments of the margin. The eastern margin displays no rift shoulder, and it is controlled by only one major normal fault, which limits the continental platform to the south, and a series of minor conjugate normal faults at the base of the continental talus.

[35] Two distinct normal fault patterns are observed in map view. The faults of the lower part

of the margin (submerged portion) are linear and consistently trend N110°E–N120°E, whereas the faults of the upper part of the margin (onshore) often have a sigmoidal shape with an overall trend of N75°E and with segments striking N70°E–N80°E and N110°E–120°E. Partitioning exists between the upper part of the margin with faults parallel to the mean trend of the Gulf of Aden, and the lower part of the margin with faults perpendicular to the opening direction of the gulf. This type of partitioning between the walls and valley of rifts has been described on axial oceanic rifts of the Reykjanes and Mohns ridges in the northern Atlantic Ocean [*McAllister et al.*, 1995; *Dauteuil and Brun*, 1996] and the Sheba Ridge in the westernmost part of the Gulf of Aden [*Dauteuil et al.*, 2001]. It is characteristic of oblique rifting. It can be interpreted as resulting from a combination of faults perpendicular to the opening direction with faults parallel to a lithospheric weakness zone (see section 7), as described by *Tron and Brun* [1991], *Dauteuil and Brun* [1993], *McClay and White* [1995], and *Clifton et al.* [2000] in their laboratory experiments. The insert in Figure 10 shows the similarity between the fault pattern in experimental clay models of oblique rifting [*Clifton et al.*, 2000] and the fault pattern observed at the northern passive margin of the Gulf of Aden. Although the age of faulting cannot be ascertained, it may be proposed that the lower margin faults, perpendicular to the opening direction, formed after the upper margin faults, when the resisting part of the lithosphere (upper mantle) had been sufficiently thinned [*Handy and Brun*, 2004]. Subsequently, the spreading segments of the Sheba Ridge formed along the same strike as the lower margin faults (N110°E–N120°E), as evidenced by the trend of the magnetic anomalies in the oldest oceanic crust. Such a scenario would agree with two diachronous extensional events during the rifting, an older N150°E–N160°E event and a younger N20°E–N30°E event, but, as stated above, our fault slip data do not provide any relative chronology between the two extension phases.

7. Discussion and Conclusion

7.1. Record of Oblique Rifting on the Passive Margin and Stress Field Evolution

[36] Fracture analysis and paleostress reconstructions along the Oman passive margin of the Gulf of Aden, in addition to an examination of the morphology of the margin onshore as well as offshore, a review of the stratigraphy and structure of the Tertiary prerift, synrift, and postrift deposits, and a compilation of AFT data from the nearby margins, bring out a coherent picture of the margin evolution since the opening of the Gulf of Aden in Oligocene times.

[37] Oblique rifting is expressed onshore and offshore by a peculiar pattern of normal faults. Rift-parallel faults along the border of the rift (upper margin) strike N70°E–N80°E, i.e., obliquely to the direction of plate divergence (N20°E), whereas faults within the rift (lower margin) trend N110°E–N120°E, i.e., perpendicular to the direction of plate divergence. This peculiarity is also reflected in the paleostress tensors reconstructed from fault slip data in Oligo-Miocene strata. Two directions of extension N150°E and N20°E can be traced along the margin from Yemen to Oman. The N150°E direction of extension reflects the predominance of the obliquity, while the N20°E direction of extension reflects the influence of the remote stress field. None of the two episodes of extension appears younger than the other, suggesting that the two are synchronous. However, it is likely that the last rifting stage (after the lithosphere had been sufficiently thinned) and subsequent spreading occurred under the influence of the dominating far-field N20°E extension.

[38] Finally, fault slip data also demonstrate the existence of a late strike-slip event which affects the whole northeastern margin of the Gulf of Aden from Dhofar to Ra's Madrakah. This event could be related to the activity of the Owen fracture zone, a right-lateral transform plate boundary between the Arabian and Indian plates since the Early Miocene, or to the Late Miocene collision of the Arabian and Eurasian plates in northern Oman.

7.2. Segmentation of the Sheba Ridge Inherited From Passive Margin Segmentation

[39] Segmentation of the margin is expressed in southern Oman by two contrasting morphotectonic segments. The western Dhofar segment is characterized by a rugged topography and the presence of synrift grabens filled with thick, deep marine deposits, whereas the eastern Jiddat Arkad segment is characterized by a gentle topography and rare synrift deposits testifying to shallow-marine deposition environments. The stress field analysis demonstrates that the two margin segments evolved under identical stress field conditions during the rifting. The segmentation of the margin appears as a local accommodation of deformation in a homo-

geneous regional stress field generated by far-field extensional forces.

[40] The boundary between the two segments is a normal fault which lies in the continuation of the Socotra transform fault. This latter crosscuts the continental crust of the lower part of the margin (depth <-2000 m), but does not crosscut the continental shelf. The fact that the Socotra fracture zone lies in the continuation of the Jiddat Arkad normal fault, and the fact that the oceanic ridge segmentation coincides in space with the passive margin segmentation, strongly suggests that the first-order segmentation of the Sheba Ridge is inherited from the prior segmentation of the passive margin.

7.3. Asymmetry of Crustal Thinning

[41] The contrasted styles of normal faulting of the two margin segments on either side of the Socotra fracture zone (cross-sections in Figure 10) show that the mechanism of rifting is different from one margin segment to the other. This difference likely reflects to the mode of crustal and lithospheric thinning during rifting, which may be either symmetric (pure-shear model [*McKenzie*, 1978]), or asymmetric (simple shear model [*Wernicke*, 1985]), or intermediate [*Brun and Beslier*, 1996]. All continental rift basins in East Africa, Gulf of Suez, Lake Baikal, or Rhine Graben are asymmetric and segmented. The asymmetry is expressed in topography, sediment thickness, structural style, and distribution of volcanics. Seismic reflection profiles revealed that rift asymmetry is controlled by crustal structures crossing the upper crust, and affecting the lower crust and possibly the Moho. During the transition to seafloor spreading, asymmetric rifts evolve into passive margins which should retain the initial asymmetry of the rift basin. A recent geophysical survey in the eastern Gulf of Aden, between the Alula-Fartak and Socotra transform faults, revealed the asymmetry of the conjugate margins [*Leroy et al.*, 2004]. The northern margin, which corresponds to our western margin segment, is shorter than the southern one and shows horsts and grabens, whereas the southern margin displays one major fault, which limits the continental shelf, and a deep basin (5200 m) at the toe of the margin. The difference between the western and eastern segments of our field area may be explained by one being the footwall and the other the hanging wall of an asymmetric set of rift basins. The segmentation of the margin thus reveals the asymmetry of the rifting process. In the absence of volcanism in the eastern Gulf of Aden, the prominent shoulder uplift of the western margin segment would be better explained if this block represents the footwall of a southward dipping normal shear zone that crosses the whole crust. The existence of a deep basin at the base of the southern conjugate margin agrees with this scheme.

[42] While continental rift basins are asymmetric, at least to the stage of development represented by the Gulf of Suez, spreading centers are generally symmetric. How can a symmetric spreading center develops in an asymmetric rift? More data concerning the deep structure of passive margins are needed to understand the latest stages of development of continental rifts and the tectonic evolution of the rift basins before seafloor spreading.

7.4. Models of Opening of the Gulf of Aden

[43] The models of oblique opening of the Gulf of Aden involve extensional boundary forces generated by the Zagros-Makran collision-subduction system (passive component), and a hot thermal anomaly in the lithosphere above the Afar mantle plume (weakness zone). Two categories of models, either with or without ridge (and rift) propagation, have been proposed. In the models without ridge propagation, the prior existence of mechanical heterogeneities in the lithosphere is invoked to explain the rifting obliquity. Several authors proposed that some of the en echelon grabens which formed the embryonic rift of the proto-Gulf of Aden, are reactivated Mesozoic grabens of similar trend known in Yemen, northern Somalia, and in the Socotra area [*Withjack and Jamison*, 1986; *Bott et al.*, 1992; *Bosence*, 1997; *Birse et al.*, 1997; *Granath*, 2001]. However, such grabens do not exist in the eastern part of the gulf, and especially on the Oman margin. Recently, *Bellahsen et al.* [2003] have shown with laboratory experiments that the interaction between far-field extensional forces and a weakness zone related to the Afar plume could produce oblique extension without the presence of defects in the continental lithosphere to explain the rift localization.

[44] In the second category of models, the ridge propagation process is responsible for the obliquity of the rifting. Following *Courtillot et al.* [1987], *Manighetti et al.* [1997] and *Courtillot et al.* [1999] related the oblique opening to the southwestward propagation of the ridge in the gulf toward the Afar mantle plume. They proposed that when the Carlsberg Ridge crossed the passive margin of the

Arabo-Somalia plate, 30 m.y. ago, it began to head for the Afar hot spot, following the shortest path across the plate. A propagation history of the Aden rift tip based on width measurements of the Gulf of Aden between continental escarpments has been proposed [*Manighetti et al.*, 1997]. The rift started to propagate about 30 m.y. ago at an average rate greater than 10 cm yr^{-1} and was arrested three times for several million years at the main fracture zones. However, the magnetic anomalies, which constitute the most reliable data to reconstruct the ridge propagation history, do not corroborate this timing. The recent works of *d'Acremont* [2002], *Huchon and Khanbari* [2003], and *Leroy et al.* [2004] show that anomaly An 5c (16 Ma) can be traced in the major part of the Gulf of Aden as far as the Shukra El Sheik discontinuity (45°E), while anomaly An 5d (18 Ma) is identified to the east of the Alula-Fartak transform fault. The ridge propagation should have been very fast and the arrests, if any, very short. As noted by *Le Pichon and Gaulier* [1988], there is no evidence for westward propagation of oceanic rifting in the main part of the Gulf of Aden and it is only in the western portion of the gulf, west of 45°E, that oceanic rift propagation toward the Gulf of Tadjura has been demonstrated [*Courtillot*, 1982; *Audin et al.*, 2001; *Hébert et al.*, 2001].

[45] To account for the two successive extension phases recognized in Yemen, *Huchon and Khanbari* [2003] used a ridge propagation model. The propagating ridge is considered as a lithospheric-scale crack propagating southwestward, under the influence of a remote N20°E extensional stress field. The younger N160°E extension, perpendicular to the ridge propagation, would result from local tensional stresses perpendicular to the propagating crack tip and is to be recorded only in the vicinity of the crack.

[46] Given the fact that (1) no definitive chronology between the N20°E and the N150°E extensions can be obtained from the study area or from the surrounding margins, and (2) no evidence for westward propagation of the ridge can be ascertained in the Gulf of Aden east of 45°E, we favor a mode of opening in which rifting and subsequent spreading took place almost simultaneously along the entire length of the main part of the gulf. As in the experiments of *Bellahsen et al.* [2003], a remotely driven extension directed along N20°E associated with a weakness zone above the Afar mantle plume led to the formation of a N75°E trending rift. The rift-bounding normal faults (upper margin) strike N75°E, whereas the normal faults inside the rift (lower margin) strike N110°E to N120°E, i.e., perpendicular to the opening direction (N20°E). This pattern of normal faults is similar to that described at oblique oceanic axial rifts and in experimental modeling studies of oblique rifting. After sufficient thinning of the resistant (mechanically brittle) part of the lithosphere (upper mantle), rifting and subsequent spreading continued under the prevailing influence of the remote N20°E extension.

Acknowledgments

[47] This study was supported by the MEBE program devoted to the Middle-East Basins Evolution. We are grateful to Cynthia Ebinger, James Cochran, and the Associate Editor John Beavan for careful reviews, and to Salim Al-Bu Saidi and Hilal Mohammed Al-Azri from the Omani Directorate General of Minerals (Ministry of Commerce and Industry) in Muscat for their support. We are indebted to Salim Al Kathiri from the Geological Survey in Salalah for his invaluable help during the fieldwork. We thank Jean-Paul Breton (BRGM, Muscat) and Jean Marcoux for their assistance. N. Bellahsen was partly supported by GDR Marges. This study greatly benefited from discussion in the field with Pépé Lepvrier and Thomas Bérard.

References

Abbate, E. P., P. Bruni, and M. Sagri (1993), Tertiary basins in the Northern Somalia continental margin: Their structural significance in the Gulf of Aden rift system, in *Geoscientific Research in Northeast Africa*, pp. 291–294, A. A. Balkema, Brookfield, Vt.

Abbate, E. P., M. L. Balestrieri, and G. Bigazzi (2001), Uplifted rift-shoulder of the Gulf of Aden in northwestern Somalia: Palinspastic reconstructions supported by apatite fission-track data, in *Peri-Tethys Memoir 6: Peri-Tethyan Rift/Wrench Basins and Passive Margins*, edited by P. A. Ziegler et al., *Mem. Mus. Natl. Hist. Nat.*, *186*, 629–640.

Abelson, M., and A. Agnon (1997), Mechanics of oblique spreading and ridge segmentation, *Earth Planet. Sci. Lett.*, *148*, 405–421.

Acocella, V., and T. Korme (2002), Holocene extension direction along the Main Ethiopian Rift, East Africa, *Terra Nova*, *14*, 191–197.

Angelier, J. (1984), Tectonic analysis of fault slip data sets, *J. Geophys. Res.*, *89*, 5835–5848.

Atwater, T., and K. C. Macdonald (1977), Are spreading centres perpendicular to their transform faults?, *Nature*, *270*, 715–719.

Audin, L., I. Manighetti, P. Tapponnier, F. Métivier, E. Jacques, and P. Huchon (2001), Fault propagation and climatic control of sedimentation on the Goubbet Rift Floor: Insights from the Tadjouraden cruise in the western Gulf of Aden, *Geophys. J. Int.*, *144*, 391–414.

Baker, J., L. Snee, and M. Menzies (1996), A brief Oligocene period of flood volcanism in Yemen: Implications for the duration and rate of continental flood volcanism at the Afro-Arabian triple junction, *Earth Planet. Sci. Lett.*, *138*, 39–55.

Béchennec, F., J. Le Métour, J. P. Platel, and J. Roger (1993), Geological map of the Sultanate of Oman, scale 1:1,000,000, Oman Minist. of Pet. and Miner., Dir. Gen. of Miner., Muscat.

Bellahsen, N., C. Faccenna, F. Funiciello, J. M. Daniel, and L. Jolivet (2003), Why did Arabia separate from Africa? Insights from 3-D laboratory experiments, *Earth Planet. Sci. Lett.*, *216*, 365–381.

Bergerat, F., A. Gudmundsson, J. Angelier, and T. Rögnvaldsson (1998), Seismotectonics of the central part of the South Iceland Seismic Zone, *Tectonophysics*, *298*, 319–335.

Beydoun, Z. R. (1970), Southern Arabia and northern Somalia: Comparative geology, *Philos. Trans. R. Soc. London, Ser. A*, *267*, 267–292.

Beydoun, Z. R. (1982), The Gulf of Aden and northwest Arabian Sea, in *The Oceans Basins and Margins*, vol. 6, *The Indian Ocean*, edited by A. E. M. Nairn and F. G. Stehli, pp. 253–313, Plenum, New York.

Birse, A. C. R., W. F. Bott, J. Morrison, and M. A. Samuel (1997), The Mesozoic and Tertiary tectonic evolution of the Socotra area, eastern Gulf of Aden, Yemen, *Mar. Pet. Geol.*, *14*, 673–683.

Bonini, M., T. Souriot, M. Boccaletti, and J.-P. Brun (1997), Succesive orthogonal and oblique extension episodes in a rift zone: Laboratory experiments with application to the Ethiopian Rift, *Tectonics*, *16*, 347–362.

Bosellini, A. (1972), The continental margins of Somalia: Their structural evolution and sequence stratigraphy, in *Geology and Geophysics of Continental Margins*, edited by J. S. Watkins, F. Ziqiang, and K. J. McMillen, *AAPG Mem.*, *53*, 185–205.

Bosence, D. W. J. (1997), Mezosoic rift basins of Yemen, *Mar. Pet. Geol.*, *14*, 611–616.

Bott, W. F., B. A. Smith, G. Oakes, A. H. Sikander, and A. I. Ibrahim (1992), The tectonic framework and regional hydrocarbon prospectivity of the Gulf of Aden, *J. Petrol. Geol.*, *15*, 211–243.

Brun, J.-P., and M.-O. Beslier (1996), Mantle exhumation at Passive margins, *Earth Planet. Sci. Lett.*, *142*, 161–173.

Clifton, A. E., and R. W. Schlische (2003), Fracture populations on the Reykjanes Peninsula, Iceland: Comparison with experimental clay models of oblique rifting, *J. Geophys. Res.*, *108*(B2), 2074, doi:10.1029/2001JB000635.

Clifton, A. E., R. W. Schlische, M. O. Withjack, and R. V. Ackermann (2000), Influence of rift obliquity on fault-population systematics: Results of experimental clay models, *J. Struct. Geol.*, *22*, 1491–1509.

Cochran, J. R. (1981), The Gulf of Aden: Structure and evolution of a young ocean basin and continental margin, *J. Geophys. Res.*, *86*, 263–287.

Courtillot, V. (1982), Propagating rifts and continental breakup, *Tectonics*, *3*, 239–250.

Courtillot, V., A. Armijo, and P. Tapponnier (1987), Kinematics of the Sinai triple junction and a two-phase model of Arabia-Africa rifting, in *Continental Extensional Tectonics*, edited by M. P. Coward, J. F. Dewey, and P. L. Hancock, *Geol. Soc. Spec. Publ.*, *28*, 559–573.

Courtillot, V., C. Jaupart, I. Manighetti, P. Tapponnier, and J. Besse (1999), On causal links between flood basalts and continental breakup, *Earth Planet. Sci. Lett.*, *166*, 177–195.

d'Acremont, E. (2002), De la déchirure continentale à l'accrétion océanique: Ouverture du golfe d'Aden oriental, Ph.D. thesis, 330 pp., Univ. of Paris 6, Paris.

Dauteuil, O., and J. P. Brun (1993), Oblique rifting in a slow-spreading ridge, *Nature*, *361*, 145–148.

Dauteuil, O., and J. P. Brun (1996), Deformation partitionning in a slow-spreading ridge undergoing oblique extension (Mohns Ridge, Norvegian Sea), *Tectonics*, *17*, 303–310.

Dauteuil, O., P. Huchon, F. Quemeneur, and T. Souriot (2001), Propagation of an oblique spreading centre: The western Gulf of Aden, *Tectonophysics*, *332*, 423–442.

Eyal, Y. (1996), Stress field fluctuations along the Dead Sea rift since the middle Miocene, *Tectonics*, *15*, 157–170.

Fantozzi, P. L. (1996), Transition from continental to oceanic rifting in the Gulf of Aden: Structural evidence from field mapping in Somalia and Yemen, *Tectonophysics*, *259*, 285–311.

Fournier, M., O. Fabbri, J. Angelier, and J. P. Cadet (2001a), Kinematics and timing of opening of the Okinawa Trough: Insights from regional seismicity and onland deformation in the Ryukyu arc, *J. Geophys. Res.*, *106*, 13,751–13,768.

Fournier, M., P. Patriat, and S. Leroy (2001b), Reappraisal of the Arabia-India-Somalia triple junction kinematics, *Earth Planet. Sci. Lett.*, *184*, 103–114.

Garcia, S., J. Angelier, F. Bergerat, and C. Homberg (2002), Tectonic analysis of an oceanic transform fault zone based on fault-slip data and earthquake focal mechanisms: The Húsavík-Flatey Fault zone, Iceland, *Tectonophysics*, *344*, 157–174.

Gnos, E., A. Immenhauser, and T. Peters (1997), Late Cretaceous/early Tertiary convergence between the Indian and Arabian plates recorded in ophiolites and related sediments, *Tectonophysics*, *271*, 1–19.

Granath, J. W. (2001), The Nogal rift of northern Somalia: Gulf of Aden: Reactivation of a Mesozoic rift, in *Peri-Tethys Memoir 6: Peri-Tethyan Rift/Wrench Basins and Passive Margins*, edited by P. A. Ziegler et al., *Mem. Mus. Natl. Hist. Nat.*, *186*, 511–527.

Hancock, P. L. (1985), Brittle tectonics: Principles and practice, *J. Struct. Geol.*, *7*, 437–457.

Handy, M. R., and J.-P. Brun (2004), Seismicity, structure and strength of the continental lithosphere, *Earth Planet. Sci. Lett.*, *223*, 427–441.

Hayward, N. J., and C. J. Ebinger (1996), Variations in the along-axis segmentation of the Afar Rift system, *Tectonics*, *15*, 244–257.

Hébert, H., C. Deplus, P. Huchon, K. Khanbari, and L. Audin (2001), Lithospheric structure of a nascent spreading ridge inferred from gravity data: The western Gulf of Aden, *J. Geophys. Res.*, *106*, 26,345–26,363.

Huchon, P., and K. Khanbari (2003), Rotation of the syn-rift stress field of the northern Gulf of Aden margin, Yemen, *Tectonophysics*, *364*, 147–166.

Jestin, F., P. Huchon, and J. M. Gaulier (1994), The Somalia plate and the East African rift system: Present-day kinematics, *Geophys. J. Int.*, *116*, 637–654.

Laughton, A. S. (1966), The Gulf of Aden, *Philos. Trans. R. Soc. London, Ser. A*, *259*, 150–171.

Le Pichon, X., and J.-M. Gaulier (1988), The rotation of Arabia and the Levant fault system, *Tectonophysics*, *153*, 271–294.

Lepvrier, C., M. Fournier, T. Bérard, and J. Roger (2002), Cenozoic extension in coastal Dhofar (southern Oman): Implications on the oblique rifting of the gulf of Aden, *Tectonophysics*, *357*, 279–293.

Leroy, S., et al. (2004), From rifting to spreading in the eastern Gulf of Aden: A geophysical survey of a young oceanic basin from margin to margin, *Terra Nova*, in press.

Manighetti, I., P. Tapponnier, V. Courtillot, and S. Gruszow (1997), Propagation of rifting along the Arabia-Soamalia plate boundary: The Gulfs of Aden and Tadjoura, *J. Geophys. Res.*, *102*, 2681–2710.

Mart, Y., and O. Dauteuil (2000), Analogue experiments of propagation of oblique rifts, *Tectonophysics*, *316*, 121–132.

Matthews, D. H., C. Williams, and A. S. Laughton (1967), Mid-ocean ridge in the mouth of the Gulf of Aden, *Nature*, *215*, 1052–1053.

McAllister, E., J. Cann, and S. Spencer (1995), The evolution of crustal deformation in an oceanic extensional environment, *J. Struct. Geol.*, *17*, 183–199.

McClay, K. R., and M. J. White (1995), Analogue modelling of orthogonal and oblique rifting, *Mar. Pet. Geol.*, *12*, 137–151.

McKenzie, D. P. (1978), Some remarks on the development of sedimentary basins, *Earth Planet. Sci. Lett.*, *40*, 25–32.

Menzies, M., K. Gallagher, A. Yelland, and A. J. Hurford (1997), Volcanic and nonvolcanic rifted margins of the Red Sea and Gulf of Aden: Crustal cooling and margin evolution in Yemen, *Geochim. Cosmochim. Acta*, *61*, 2511–2527.

Peters, T., and I. Mercolli (1998), Extremely thin oceanic crust in the Proto-Indian Ocean: Evidence from the Masirah Ophiolite, Sultanate of Oman, *J. Geophys. Res.*, *103*, 677–689.

Pik, R., B. Marty, J. Carignan, and J. Lavé (2003), Stability of the Upper Nile drainage network (Ethiopia) deduced from (U–Th)/He thermochronometry: Implications for uplift and erosion of the Afar plume dome, *Earth Planet. Sci. Lett.*, *215*, 73–88.

Platel, J. P., and J. Roger (1989), Evolution géodynamique du Dhofar (Sultanat d'Oman) pendant le Crétacé et le Tertiaire en relation avec l'ouverture du golfe d'Aden, *Bull. Soc. Geol. Fr.*, *2*, 253–263.

Platel, J. P., A. Berthiaux, J. Le Métour, M. Beurrier, and J. Roger (1992a), Geological map of Duqm and Madraca, Sultanate of Oman, sheet NE 40-03/07, scale 1:250,000, Oman Minist. of Pet. and Miner., Dir. Gen. of Miner., Muscat.

Platel, J. P., J. Dubreuilh, J. Le Métour, J. Roger, R. Wyns, F. Béchennec, and A. Berthiaux (1992b), Geological map of Juzor Al Halaaniyaat, Sultanate of Oman, sheet NE 40-10, scale 1:250,000, Oman Minist. of Pet. and Miner., Dir. Gen. of Miner., Muscat.

Platel, J. P., J. Roger, T. J. Peters, I. Mercolli, J. D. Kramers, and J. Le Métour (1992c), Geological map of Salalah, Sultanate of Oman, sheet NE 40-09, scale 1:250,000, Oman Minist. of Pet. and Miner., Dir. Gen. of Miner., Muscat.

Robertson, A. H. F., and K. A. S. Bamkhalif (2001), Late Oligocene-early Miocene rifting of the northeastern Gulf of Aden: Basin evolution in Dhofar (southern Oman), in *Peri-Tethys Memoir 6: Peri-Tethyan Rift/Wrench Basins and Passive Margins*, edited by P. A. Ziegler et al., *Mem. Mus. Natl. Hist. Nat.*, *186*, 641–670.

Roger, J., J. P. Platel, C. Cavelier, and C. Bourdillon-de-Grisac (1989), Données nouvelles sur la stratigraphie et l'histoire géologique du Dhofar (Sultanat d'Oman), *Bull. Soc. Geol. Fr.*, *2*, 265–277.

Roger, J., J. P. Platel, A. Berthiaux, and J. Le Métour (1992), Geological map of Hawf with explanatory notes, sheet NE 39-16, scale 1:250,000, Oman Minist. of Pet. and Miner., Dir. Gen. of Miner.

Sahota, G. (1990), Geophysical investigations of the Gulf of Aden continental margins: Geodynamic implications for the development of the Afro-Arabian Rift System, Ph.D. thesis, Univ. of Wales, Swansea.

Sandwell, D. T., and W. H. F. Smith (1997), Marine gravity anomaly from Geosat and ERS-1 satellite altimetry, *J. Geophys. Res.*, *102*, 10,039–10,054.

Tamsett, D. (1984), Comments on the development of rifts and transform faults during continental breakup; examples from the Gulf of Aden and northern Red Sea, *Tectonophysics*, *104*, 35–46.

Tamsett, D., and R. C. Searle (1988), Structure and development of the midocean ridge plate boundary in the Gulf of Aden: Evidence from Gloria side scan sonar, *J. Geophys. Res.*, *93*, 3157–3178.

Tron, V., and J.-P. Brun (1991), Experiments on oblique rifting in brittle-ductile systems*Tectonophysics*, *188*, 71–84.

Tuckwell, G. W., J. M. Bull, and D. J. Sanderson (1996), Models of fracture orientation at oblique spreading centres, *J. Geol. Soc. London*, *153*, 185–189.

Tuckwell, G. W., J. M. Bull, and D. J. Sanderson (1998), Numerical models of faulting at oblique spreading centers, *J. Geophys. Res.*, *103*, 15,474–15,482.

Ukstins, I. A., P. R. Renne, E. Wolfenden, J. Baker, D. Ayalew, and M. Menzies (2002), Matching conjugate volcanic rifted margins: $^{40}Ar/^{39}Ar$ chrono-stratigraphy of pre- and syn-rift bimodal flood volcanism in Ethiopia and Yemen, *Earth Planet. Sci. Lett.*, *198*, 289–306.

Watchorn, F., G. J. Nichols, and D. W. J. Bosence (1998), Rift-related sedimentation and stratigraphy, southern Yemen (Gulf of Aden), in *Sedimentation and Tectonics of Rift Basins: Red Sea-Gulf of Aden*, edited by B. H. Purser and D. W. J. Bosence, pp. 165–191, Chapman and Hall, New York.

Wernicke, B. (1985), Uniform-sense normal simple shear of the continental lithosphere, *Can. J. Earth Sci.*, *22*, 108–125.

Wilson, T. W. (1965), A new class of faults and their bearing on continental drift, *Nature*, *207*, 343–347.

Withjack, M. O., and W. R. Jamison (1986), Deformation produced by oblique rifting, *Tectonophysics*, *126*, 99–124.

Zoback, M. L. (1992), First-and second-order patterns of stress in the lithosphere: The World Stress Map Project, *J. Geophys. Res.*, *97*, 11,703–11,728.